

Deanship of Graduate Studies
Al – QudsUniversity



Study The Interaction Of Retinol (Vitamin A₁) With
HSA Using Spectroscopic Techniques

Riziq Salman Aldrabee'

M.Sc. Thesis

Jerusalem – Palestine

1439 / 2017

Deanship of Graduate Studies
Al – Quds University



Study The Interaction Of Retinol (Vitamin A₁) With
HSA Using Spectroscopic Techniques

Prepared by:
Riziq Salman Aldrabee'

Supervisor: Prof. Dr. Musa Abu-Teir

A thesis submitted in partial fulfillment of requirement
for the degree of Master of Science in Physics

Jerusalem – Palestine

1439/2017

Deanship of Graduate Studies
Al – Quds University



Thesis Approval

Study The Interaction Of Retinol (Vitamin A₁) With HSA Using Spectroscopic Techniques

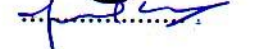
Prepared by: Riziq Salman Aldrabee'
Registration No: 21220329

Supervisor: Prof. Dr. Musa Abu Teir

Master thesis submitted and accepted, date 05 / 01 / 2018

The name and signature of examining committee member are as follows:

- 1- Head of the committee: Prof. Musa Abu Teir
2. Internal Examiner: Dr. Husain Alsamamra
3. External Examiner: Dr. Jamal Ghabbon

Signature: 
Signature: 
Signature: 

Jerusalem – Palestine

1439/2017

Dedication

I dedicate this project to God Almighty, my Creator, my strong call, the source of my inspiration, Wisdom, knowledge and understanding.

I devoted this thesis to all my wonderful family members who supported me during my life and allowed me to achieve my goals: to my father who helped make my educational decisions and sent me on the road to my higher career; to my mother; who raised me to be the person I am today.

You have been with me in every step of the way, through good and bad times. Thank you for all the unconditional love, guidance, and support that you have always given me, helping me succeed and instilling in me the confidence that I am capable of doing anything I put my mind to. To the loyal brothers. To the nice sisters. And a great thank you to my wife(tahani) for her support and encouragement to me throughout my life

A special dedication to my teachers, I will always appreciate every encouraging word I have been told throughout my life. I also dedicate my work to my colleagues I met in the educational and professional career of my life. I appreciate their support from my heart. I dedicate this work to everyone who respects my position and believes in me and a great thank you to everyone who has been and remains special to me at any stage of my life. I love you all.

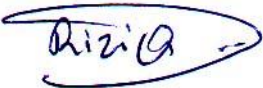
Riziq Salman Aldrabee'

Declaration

I certify that this thesis submitted for the degree of master is the result of my own research, except where otherwise acknowledged, the present thesis or any part of it has not been submitted for a higher degree to any other university or institution.

The work was done under the supervision of Prof. Dr. Musa Abu Teir , at Al – QudsUniversity, Palestine.

Name: Riziq Salman Aldrabee'

Signed: 

Date: 23 / 12 / 2017

Acknowledgements

Always the first and last great thanks is to Allah, who gave me the ability and energy to accomplish this work, all this work would not have taken place without his blessing. Thanks to Allah for all his graces upon us Great thanks for everyone who have taught me a word during my educational. Thanks for being generous with your expertise and precious time.

Many thanks to my advisors; Prof. Dr. Musa Abu Teir and Dr . Hussein Sammara, whom helped me to achieve my dream, to work in Biophysics field and for their help and encouragements during my work. Also I would like to thank Prof. Dr. Saker Darwish for his help . Lot of thanks go for the Nano-Technology Lab group; Maryam in particular, for their help and encouragements. Of course, I am grateful to my parents for their patience and love. Without them this work would never have come into existence.

Riziq Salman Aldrabee'

Abstract

It was found that the distribution and metabolism of many biologically active compounds in the body whether vitamins, drugs or natural products are correlated with their affinities toward serum albumin. Thus, studying the interaction of such molecules with albumin is an imperative and fundamental importance. Extensive studies of different aspects of Retinol (Vitamin A₁)–HSA interactions are still in progress because of the clinical significance of the processes. In this study, the interaction between Retinol and HSA has been investigated using Ultraviolet and visible (Uv-vis) absorption spectrophotometry, fluorescence spectroscopy and Fourier Transform Infrared (FT-IR) spectroscopy: binding constant and the effects on the protein secondary structure have been confirmed.

The values of the binding constants for Retinol (vitamin A₁) : HSA mixtures by using Ultraviolet and visible (Uv-vis) absorption spectrophotometry and fluorescence spectroscopy are calculated at room temperature (293K) found to be: ($1.7176 \times 10^2 \text{ M}^{-1}$) and ($1.32 \times 10^2 \text{ M}^{-1}$), respectively, In addition, the Stern-Volmer constant and quenching rate constant are calculated ($1.885 * 10^2 \text{ L. M}^{-1}$) and ($1.885 * 10^{10} \text{ L Mol}^{-1} \text{ s}^{-1}$), respectively. From UV-VIS absorption spectrophotometry which showed an increase in the absorption intensity with increasing the molecular ratios of Retinol (concentration) to HSA, while the concentration of the protein (HSA) remained constant. Using the fluorescence spectroscopy, the intensity of radiation emitted by Retinol (vitamin A₁) reaction with HSA decreased by increasing the concentration of Retinol (vitamin A₁) and while the concentration of the protein (HSA) remained constant. This increase in the intensity of the emitted radiation indicates retinol (vitamin A₁) has a strong ability to increase or raise the self-emitting radiation of the human blood protein (HSA) through the mechanism (static quenching).

Using FT-IR spectroscopy with Fourier self-deconvolution technique and second derivative resolution enhancement procedures and curve fitting technique were applied in the analysis of the amide I, II, and III regions to determine the protein secondary structure and retinol (vitamin A₁) binding mechanism with blood protein (HSA). It has been observed that with the increase of retinol (vitamin A₁) concentrations to the blood protein (HSA), absorption bands decrease. All peaks positions in the three amide regions (amide I, amide II and amide III) were identified at various ratios of retinol (vitamin A₁) compared to human blood protein (HSA). In addition, The FTIR spectra measurements indicate a change in the intensity of absorption bands is due to change in the concentrations of retinol. and larger intensities decrease in the absorption band of α -helix relative to that of β -sheets has been observed. This variation in intensity is related indirectly to the formation of H-bonding in the complex molecules, which accounts for the different intrinsic propensities of α -helix and β -sheets.

Table of Contents

Abstract.....	vi
List of Tables	ix
List of Figures.....	x
List Of abbreviations:.....	xii
List Of Symbols:.....	xiii
Introduction	2
Background and Theoretical Considerations	6
2.1 Electromagnetic Waves (EMW)	6
2.2 Vibrational spectroscopy.	9
2.2.1 Normal modes of vibrations:.....	10
2.2.2 Quantum mechanical treatment of vibrations:	11
2.3 Spectroscopy.....	13
2.3.1 Infrared spectroscopy:.....	13
2.3.2 Fourier transforms infrared spectroscopy (FTIR):.....	14
2.3.3 Ultraviolet-Visible Spectroscopy (UV-vis):	18
2.3.4 Fluorescence:	20
2.3.5 Fluorescence Quenching:	21
2.4 Proteins	22
2.4.1 Protein Structure:	22
2.5 Human Serum Albumin (HSA).....	28
2.6 Retinol (Vitamin A ₁).....	29
Experimental part	31
3.1 Samples and materials.....	31
3.1.1 Preparation of HSA stock solution:.....	31
3.1.2 Preparation of Retinol (Vitamin A ₁) stock solution:.....	31
3.1.3 HSA- Retinol (Vitamin A ₁) samples:.....	31
3.1.4 Thin film preparations:.....	31
3.2 Instruments.....	32
3.2.1 FT-IR Spectrometer:	32
3.2.2 UV-VIS spectrophotometer (NanoDrop ND-1000):.....	32

3.2.3 Fluorospectrometer (NanoDrop 3300):.....	32
3.3 Experimental procedures	32
3.3.1 UV-VIS Spectrophotometer experimental procedures:	32
3.3.2 Fluorospectrometer experimental procedures:	33
3.3.3 FT-IR Spectrometer experimental procedures:	34
3.3.3.1 FT-IR data processing:	34
Results and Discussion	37
4.1 UV-absorption spectroscopy.....	37
4.1.1 Binding constants of retinol complexes using UV-VIS Spectrophotometer:	38
4.2 Fluorescence spectroscopy.....	39
4.2.1 Determination of Stern-Volmer quenching constants (K_{sv}) and the quenching rate constant (K_q):.....	39
4.2.2 Determination of the binding constants (K) by fluorescence spectroscopy for HAS -Retinol ..	41
4.3 FT-IR Spectroscopy	42
4.3.1 Peak positions:	43
4.3.2 Secondary structural changes:.....	46
Conclusions and future work	51
المخلص.....	57

List of Tables

Table 2.1: Degrees of freedom for polyatomic molecules	11
Table 2.2 Characteristic amide bands of peptide linkage.	17
Table 2.3 Deconvoluted amide I band frequencies and assignments to secondary structure for protein in D ₂ O and H ₂ O media.	18
Table 2.4 Absorption characteristics of some common chromophoric groups.	20
Table 4.1 Band assignment in the absorbance spectra of HSA with different Retinol molecular ratios for amide I, amide II, and amide III region..	45
Table 4.2 Secondary structure determination for the free HSA and its Retinol mixture for amide I , amide II , amide III.	48

List of Figures

Figure 1.1 Chemical structure of human serum albumin	2
Figure 2.1: The electromagnetic spectrum.....	7
Figure 2.2: A schematic representation of the quantized electronic and vibrational energy levels of a molecule.....	8
Figure 2.3: A setup of an absorption measurement.....	8
Figure 2.4: Diatomic molecule as a mass on a spring.....	10
Figure 2.5: potential energy of a diatomic molecule as a function of atomic displacement (inter-nuclear separation) during vibration. The Morse potential (blue) and harmonic oscillator potential (green) (Wikipedia: Vibronic spectroscopy).	12
Figure 2.6: Intramolecular hydrogen bonding in a protein	13
Figure 2.7: Effect of hydrogen bonding on an O–H stretching vibration	14
Figure 2.8: Incident and transmitted IR-radiation upon passing through a sample.	14
Figure 2.9: Michelson interferometer	16
Figure 2.10: the layout and the main components of FTIR.	16
Figure 2.11: Generalized molecular orbital energy level diagram and possible transitions for organic compounds	19
Figure 2.12: Absorption ranges for various electronic transitions.....	19
Figure 2.13: Amino acid structure.	22
Figure 2.14: Alpha Helix Protein.....	23
Figure 2.15: Beta Pleated Sheet	24
Figure 2.16: Anti parallel Beta Pleated Sheet Protein.....	24
Figure 2.17: Parallel Beta Pleated Sheet Protein	24

Figure 2.18: Chemical structure of Retinol (vitamin A ₁).....	29
Figure 3.1: Main steps for using the sample fluorospectrophotometer (NanoDrop 3300)	33
Figure 4.1: UV-Absorbance spectra of HSA with different molar ratios of retinol, HSA: retinol (a=1:0, b=1:1, c=1:2, d=1:5, e=1:10, f=1:20), no UV absorption for retinol.	37
Figure 4.2: The plot of 1/(A-A ₀) vs. 1/L for HSA with different concentrations of retinol.	38
Figure 4.3: The fluorescence emission spectra of HSA with various concentrations of Retinol (a=1:0, b=1:1, c=1:2, d=1:5, e=1:10, f=1:20).....	39
Figure 4.4: The plot of F ₀ /F vs [L] for HSA- Retinol	40
Figure 4.5: The plot of 1/(F ₀ -F) vs 1/L for HSA- Retinol complexes.	41
Figure 4.6: Sample spectrum showing the three relevant regions for determination of protein secondary structure. Amide I (1700-1600 cm ⁻¹), amide II (1600-1480 cm ⁻¹) and amide III (1330-1220 cm ⁻¹) (Vonhoff et al., 2010).....	42
Figure 4.7: The spectra of HSA free (second derivative)..	43
Figure 4.8: (a, b, c, d, e, f) Retinol -HSA with ratios (0:1, 1:1, 2:1, 5:1, 10:1, 20:1), respectively.	43
Figure 4.9: FTIR spectra (top two curves) and difference spectra [(protein solution+ Retinol solution)-(protein solution)] (bottom five curves) of the free human serum albumin (HSA) and its Retinol complexes in aqueous solution..	45
Figure 4.10: Second-derivative enhancement and curve-fitted Amide I region (1600-1700 cm ⁻¹) and secondary structure determination of the free human serum albumin (A and B) and its Retinol mixture(C and D) with 20: Retinol: HSA ratios.....	49

List Of abbreviations:

Symbol	Abbreviation representation
A	Absorbance
C	Concentration
Diff	Difference
EM	Electromagnetic
Eq.	Equation
FSD	Fourier self deconvolution
FT-IR	Fourier Transform Infrared
HSA	Human Serum Albumin
IR	Infra-red
kDa	kilodalton
LED's	Light emitting diodes
Mid-IR	Middle infrared
MIR	Magnetic Imaging Resonance
MRI	Magnetic resonance image
nm	nanometer
OPUS	Optical User Software
PET	Positron Emission Tomography
pH	Power of hydrogen
T	Transmittance
UV-VIS	Ultraviolet –visible light
Vit.A ₁	Retinol
α -helix	alpha helix
β -sheets	Beta sheets

List Of Symbols:

Symbol	Abbreviation representation
[L]	The quencher concentration.
a	Constant for a particular molecule.
A	The recorded absorption at different Testosterone concentrations (L).
A_0	The initial absorption of protein at 280 nm in the absence of ligand
A_∞	The final absorption of the ligated protein
B	The path length
C	Speed of light
D_{eq}	The dissociation energy.
E_{total}	Total energy
E_{ele}	Electronic energy
$E_o(v)$	The maximum amplitude of the beam at $z=0$
E_{rot}	Rotational energy
E_v	The potential energy for harmonic oscillator approximation
E_{vib}	Vibrational energy
F	Fluorescence intensity with quencher
f	The spring or force constant
F_0	Fluorescence intensity without quencher
F_x	Restoring force acts on the spheres
h	Planck's constant
$h\nu_{EM}$	Energy of photon emitted
$h\nu_{EX}$	The excitation photon energy
$I(z_1, z_2, v) dv$	The intensity after recombination of the beams for the fixed spectral range dv
I_0	The radiant power incident on the sample
K	Binding constant
K_{sv}	The Stern-Volmer quenching constant
m_A, m_B	Mass of particles A,B
$S(v)$	The spectrum
S_0	The ground singlet electronic state
S_1 and S_2	The successively higher energy excited singlet electronic states
T	The kinetic energy of the oscillating motion

T_1	The lowest energy triplet state
V	The potential energy
$\tilde{\nu}$	Circular frequency in wave-numbers
V	Vibrational level
ω_e	Oscillating frequency
$\hat{\omega}_e$	Oscillation frequency in wave number
X_e	The an-harmonicity constant
Δ	Un-saturation site
Δx	Displacement of the spheres along the x-axis from equilibrium position
ϵ	molar extinction coefficient
λ	Wavelength
μ	The reduced mass
ν	Frequency
τ	The unquenched lifetime
k_q	The bimolecular quenching constant
ω	Circular frequency of the harmonic vibration

Chapter One

Introduction

Chapter One

Introduction

Of all the molecules encountered in living organisms, proteins are the most abundant and diverse from a functional point of view. From the hormones and enzymes that control metabolism, the framework forming collagen in bones, the contractile proteins in muscles, to the haemoglobin and albumin in the bloodstream and immunoglobulins fighting infections, almost every life process relies on this class of molecules (Beharka, A., et al., 1997).

Albumin is the most abundant protein in the vertebrates' organisms (up to 40 mg/ml) and the most prominent plasma protein (about 60% of the total protein content of plasma) (Norman. A.W., et al. 2004). It is one of the first discovered and most intensely studied proteins (Tushar,K.M., et al. 2008). .

The investigation of the binding amplitude and mechanism of interaction of small molecules with serum albumins is crucial for the understanding of drug pharmacodynamics and pharmacokinetics, as the nature and strength of that interaction has a great influence on drug absorption, distribution, metabolism and excretion (Ouameur,A., et al. 2004; Ji-Sook, Ha.A., et al. 2006; Abu Teir, M., et al. 2010; Abu Teir, M. M., et al. 2014; Darwish, S. M., et al. 2010).

This research is concerned with using spectroscopic techniques such as Fourier Transform Infrared Spectroscopy (FTIR), UV-Vis spectroscopy, Fluorescence spectroscopy to investigate the effect of Retinol on Human serum albumin(HSA).

Human serum albumin (HSA) is the most abundant protein in blood plasma and is able to bind and thereby transport various compounds such as fatty acids, hormones, bilirubin, tryptophan, steroids, metal ions, therapeutic agents and a large number of drugs. HSA serves as the major soluble protein constituent of the circulatory system, it contributes to colloid osmotic blood pressure, it can bind and carry drugs which are poorly soluble in water (Abu Teir, M., et al. 2010). It is a globular protein consisting of a single peptide chain of 585 amino acids. This protein composed of three structurally similar domains (labeled as I, II, III) (Cui,A., et al. 2008; Kang, J., et al. 2004; Rondeau, P.A., et al. 2007; Abu Teir, M., et al. 2010). Each containing two sub domains (A & B) having six and four α -helices, respectively. See Figure (1.4).

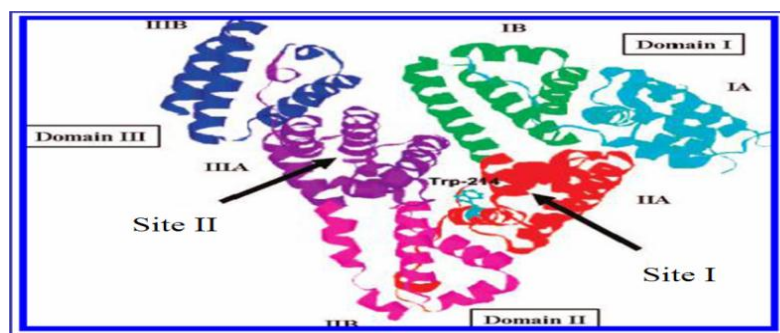


Figure 1.1 : Chemical structure of human serum albumin (Abou-Zied, K., et al. 2009).

Retinol, also known as Vitamin A₁, is a vitamin found in food and used as a dietary supplement. As a supplement it is used to treat and prevent vitamin A deficiency, especially that which is resulting in xerophthalmia. In areas where deficiency is common a single large dose is recommended to those at high risk a couple of times a year. It is also used to prevent further issues in those who have measles. It is used by mouth or injection into a muscle (Bates, CJ. et al. 1995).

Retinol at normal doses is well tolerated. High doses may result in an enlarged liver, dry skin, or hypervitaminosis A. High doses during pregnancy may result in harm to the baby. Retinol is in the vitamin A family. It or other forms of vitamin A are needed for eye sight, maintenance of the skin, and human development. It is converted in the body to retinal and retinoic acid through which it acts. Dietary sources include fish, dairy products, and meat (Smith, FR, Goodman, DS. 1976).

The first spectroscopic technique that is used in the process is FTIR which is used in order to investigate the conformational changes on the secondary structure of HSA upon the addition of different concentrations of Retinol on it.

Investigation of structural changes includes changes in peak positions and changes in the relative intensities of the secondary structural elements are performed. Also the effect of temperature on HSA - free, HSA - Retinol complex are examined.

UV-absorption spectroscopy is the second spectroscopic technique that is used to investigate the strength of interaction between HSA with Retinol. The binding constant between the ligands and HSA will be determined.

Fluorescence spectroscopy was used to confirm the calculation of binding constants as an indication of the strength of interaction. The Stern- Volmer quenching constants for Retinol interaction with HSA will also be calculated.

The **first** chapter is an introduction. It contains the purpose and the importance of this work. It also gives information about each chapter in this thesis.

In the **second** chapter of this thesis, the physical background and theoretical considerations of spectroscopy will be discussed, then a brief introduction to spectroscopic technique used in this research will be given. A brief introduction to proteins, their structural levels, and protein misfolding are given , then information about materials being used (Retinol, HSA) are given.

In chapter **three** the experimental part of the study is discussed in details. Sample preparation from the moment of taking the solid protein sample to the moment of inserting the sample inside FTIR equipment is explained. A brief discussion of the instruments is given, and then the experimental procedure followed in taking the needed data is mentioned.

In chapter **four** results are analyzed and discussed. The UV-absorption spectroscopy results are plotted and used to calculate the binding constant between HSA and Retinol. The absorption spectra of HSA with different concentrations of Retinol are shown.

A plot of the fluorescence emission spectra of HSA in the absence and presence of Retinol are shown. The binding constant, Stern-Volmer quenching constants and the quenching rate constant of the bio-molecule will be calculated.

FTIR shows Changes in amide I and e II peaks positions for HSA with different concentrations of Retinol are investigated, also changes in the intensity of the component bands of the secondary structure as a result of concentrations of Retinol have been shown. The effect of changing temperature on the peak positions and on the intensity of β -sheet bands for HSA free, HSA - Retinol complex have been examined.

The **last** chapter contains the conclusion and recommends future work that can be done in this field.

Chapter Two

Background and Theoretical Considerations

Chapter two

Theoretical Background

Biophysics is an interdisciplinary science that applies the approaches and methods of physics to study biological systems. Biophysics covers all scales of biological organization, from molecular to organismic and populations. Biophysical research shares significant overlap with biochemistry, physical chemistry, nanotechnology, bioengineering, computational biology, biomechanics and systems biology. Biophysics contributes to the development of medical imaging technologies including magnetic resonance image (MRI), computer assisted tomography scanning (CAT), PET scans, Fourier transform (FT-IR), UV-VIS and fluorescence spectrophotometers. Advanced biophysical research instruments are the daily workhorses of drug development in the world's pharmaceutical and biotechnology industries. Spectrophotometers are powerful tools for studying biological samples such as proteins(Ouameur, A., et al. 2004; Ji-Sook, Ha.A., et al. 2006; Abu Teir, M. M., et al. 2014; Darwish, S. M., et al. 2010) .

This chapter will cover theoretical aspects of this work, the first two sections will include a short historical background on the development of FT-IR spectroscopy and electromagnetic spectrum, next section will cover briefly molecular vibrations, the following three sections discuss the spectroscopic approaches used in this work; FT-IR, UV-VIS, and fluorescence spectrophotometers. Final section will include protein structure and the protein model that have been used in this work which is "Human Serum Albumin (HSA)"and Retinol (Vitamin A₁).

2.1 Electromagnetic waves (EMW)

Electromagnetic waves (EMW) are transverse oscillating waves composed of electric and magnetic fields perpendicular to each other and perpendicular to the direction of propagation. EMW propagate as a sine or cosine waves at the speed of light in vacuum (Stuart, B. 2004).

The electromagnetic spectrum consists of radio waves, microwaves, infrared radiation, visible light, ultraviolet radiation, X-rays and gamma rays as show in (Figure 2.1).

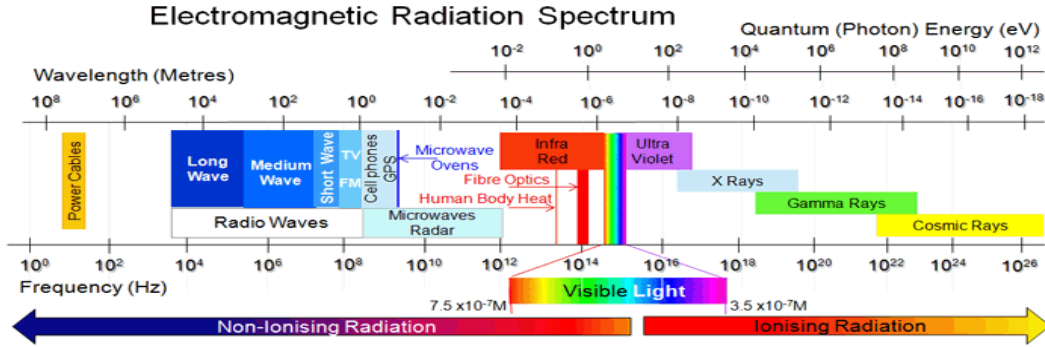


Figure 2.1: The electromagnetic spectrum (Sharma, B.K. 2007, Ball, D.W. 2001).

Wavelength (λ) is inversely proportional to frequency(ν) and it is governed by the relation:

$$\lambda = \frac{c}{\nu} \quad (1)$$

Where c is speed of light and ν is the frequency.

Electromagnetic radiation is composed of multiple electromagnetic waves or photons, which carry energy, momentum and angular momentum.

The energy of each photon is given by Planck–Einstein equation:

$$E = h \nu = h \frac{c}{\lambda} \quad (2)$$

Where E is the energy, h is Planck's constant, ν is frequency, and λ is wavelength (Pavis, D. et al 2008, Yadav, L.D. 2005, Williams, D. 1976, Ball, D.W. 2001).

The atomic spectra arise from the transition of electron between atomic energy levels, while molecular spectra arise from three types of energy transitions due to molecular rotation, molecular vibrational, and electronic transition. According to Born Oppenheimer approximation, the total energy of the molecule is given by :

$$E_{\text{total}} = E_{\text{rot}} + E_{\text{vib}} + E_{\text{el}} \quad (3)$$

Where: E_{rot} : is rotational energy due to the molecule rotation about the axis passing the center of gravity for the molecule.

E_{vib} : is vibrational energy due to the periodic displacement of atoms around their equilibrium positions.

E_{el} : is related to the energy of the molecule's electrons (Sharma, B.K. 2007).

When radiation falls on a sample it may be absorbed, this occur when the energy of radiation matches the difference in energy levels of the sample, otherwise it may be either transmitted or scattered by the sample. A simplified representation of the quantized electronic and vibrational states is represented in (Fig 2.2). It is clear that transitions between electronic energy states require more energy than transitions between vibrational energy states (Hollas, J. 2004, Turro, N.J. 1991, Ball, D.W. 2001).

IR radiation does not have enough energy to induce electronic transitions as seen with UV and visible light. Absorption of IR is appropriate to excite vibrational and rotational states of a molecule as shown in (Fig 2.1)

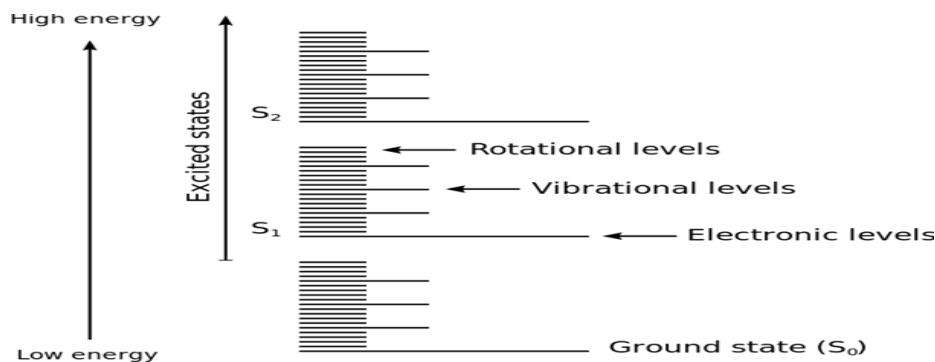


Figure 2.2: A schematic representation of the quantized electronic and vibrational energy levels of a molecule.

Intensity of the light absorbed to produce a given transition is given by Beer-Lambert law:

$$\frac{I}{I_0} = 10^{-\epsilon c l} \quad (4)$$

In which I and I_0 are the intensity of light transmitted through the absorber and incident upon it respectively, ϵ : is the molar absorption coefficient or (molar extinction coefficient), c : is the concentration of absorbing molecule in the sample, and l : is the length of the light path in the sample. The above equation can be represented in logarithmic form:

$$A = \log_{10} \left(\frac{I_0}{I} \right) = \epsilon(v) c l \quad (5)$$

Where A is called Absorbance (Hollas, J. 2004, Schulman, S.G. 1977). A setup for an absorption instrument is shown in (Fig 2.3).

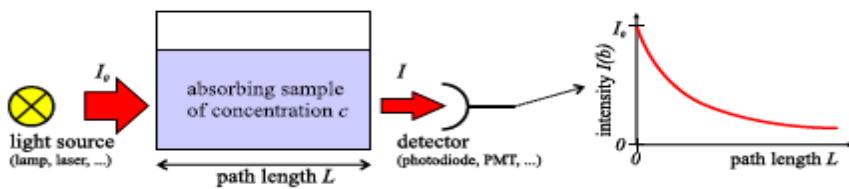


Figure 2.3: A setup of an absorption measurement

2.2 Vibrational spectroscopy

Infrared spectroscopy provides measurements of molecular vibrations due to the specific absorption of infrared radiation by chemical bonds (Narhi, L.O. 2013). The energy at which peak in absorption spectrum appears corresponds to a frequency of vibration of a part of a sample molecule. As the starting point for introducing the concept of harmonic vibrations, it is instructive to consider molecules as an array of point masses that are connected with each other by mass-less springs representing the intra-molecular interactions between the atoms (Wilson, E., et al. 1955).

The simplest case is given by two masses, m_A and m_B , corresponding to diatomic molecule A-B upon displacement of the spheres along the x-axis from equilibrium position by Δx , a restoring force F_x acts on the spheres, which according to Hooke's law, is given by

$$F_x = -f\Delta x \quad (6)$$

Here f is the spring or force constant, which is a measure of the rigidity of the spring, that is, the strength of the bond (Hildebrandt, P., et al. 2008).

The potential energy V depends on the square of the displacement from the equilibrium position,

$$V = \frac{1}{2} f \Delta x^2 \quad (7)$$

As when spring (bond) is stretching it will affect the equilibrium distance (bond length) so potential energy will be affected.

The kinetic energy T of the oscillating motion is:

$$T = \frac{1}{2} \mu (\Delta \dot{x})^2 \quad (8)$$

Where μ is the reduced mass defined by:

$$\mu = (m_A \cdot m_B) / (m_A + m_B) \quad (9)$$

Because of the conservation of energy, the sum of V and T must be constant such that the sum of the first derivatives of V and T is equal to zero. This leads eventually to the Newton equation of motion:

$$\frac{d^2 \Delta x}{dt^2} + \frac{f}{\mu} \Delta x = 0 \quad (10)$$

This equation represents the differential equation for a harmonic motion. Solving this equation leads to:

$$\omega = \sqrt{\frac{f}{\mu}} \quad (11)$$

The above equation describes what one intuitively expects that the circular frequency of the harmonic vibration increases when rigidity of the spring (or the strength of the bond) increases but decreases with increasing masses of the atoms (spheres). In order to express the circular frequency in wave-numbers (in cm^{-1}) can be divided by $2\pi c$,

$$\nu = \frac{1}{2\pi} \pi c \sqrt{\frac{f}{\mu}} \quad (12)$$

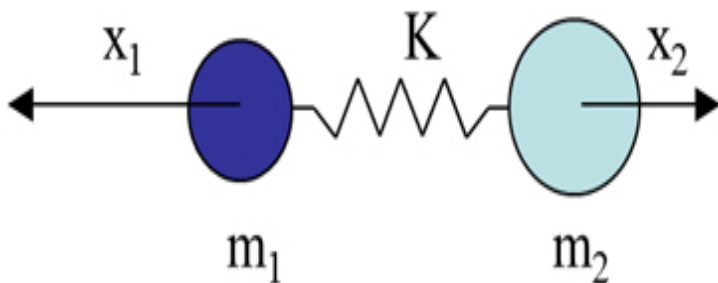


Figure 2.4: Diatomic molecule as a mass on a spring (bwtek.com).

2.2.1 Normal modes of vibrations

The normal modes of a system are the vibrational motions of the system, such that each coordinate of the system oscillates under simple harmonic motion with the same frequency (Rosman, B. 2008). In Cartesian coordinate system, each atom can be displaced in the x-, y- and z-directions, corresponding to three degrees of freedom. Thus, a molecule of N atoms has in total $3N$ degrees of freedom, but not all of them correspond to vibrational degrees of freedom. It can be seen easily that a nonlinear molecule (where the atoms are not located in straight line) has three rotational degrees of freedom, whereas there are only two for a linear molecule. The remaining $3N-6$ and $3N-5$ degrees of freedom correspond to the vibrations of a nonlinear and a linear molecule, respectively (Hildebrandt, P., et al. 2008).

Table 2.1: Degrees of freedom for polyatomic molecules (Stuart, B. 1997).

Type of degrees of freedom	Linear	Non-linear
Translational	3	3
Rotational	2	3
Vibrational	3N-5	3N-6
Total	3N	3N

Stretching and bending are two types of molecular vibrations correspond to the normal mode of molecule. Stretching is rhythmical movement along the bond axis and can be symmetric or anti-symmetric. Bending vibrations arise from a change in bond angle between two atoms or movement of a group of atoms, relative to the remainder of the molecule (Mirabeela, F.M. (ED). 1998). The frequency of normal modes is a characteristic of the presence of certain functional group by examination of this frequency one can determine which functional groups are present or absent (Shernan, M . 2014). Many of the group frequencies vary over a wide range because the bands arise from complex interacting vibrations within the molecule. Absorption bands may, however, represent predominantly a single vibrational mode. Certain absorption bands, for example, those arising from C-H, O-H, and C=O stretching modes, remain within fairly narrow regions of the spectrum.

2.2.2 Quantum mechanical treatment of vibrations

I. The harmonic oscillator approximation treats a diatomic as if the nuclei were held together by a spring. The potential energy of classical harmonic oscillator depends upon the square of the displacement from equilibrium and the strength of the spring. All values of energy are allowed classically. The quantum mechanical solution to the harmonic oscillator equation of motion predicts that only certain energies are allowed, (Griffith, P. & Haseth, J. 2007).

$$E_v = \frac{h}{2\pi} \sqrt{\frac{f}{\mu}} \left(v + \frac{1}{2} \right) \quad (13)$$

The potential energy for diatomic molecule for harmonic oscillator approximation is shown below in figure 2.5.

II. The an-harmonic oscillator

Real molecules do not obey exactly the simple harmonic motion, real bonds do not follow Hooke's law they are not so elastic. If for example a bond stretches of 60% of its real length then a molecular complicated situation should be assumed.

The Morse curve, for a molecule undergoing on harmonic extensional compression a purely empirical expression which fits this curve to good approximation was derived by P. Morse and is called the Morse function (Morse, P. M. 1929) :

$$E = D_{eq} [1 - \exp(-a(r_{eq} - r))]^2 \quad (14)$$

a = constant for a particular molecule.

D_{eq} = the dissociation energy.

When it is treated using Schrodinger equation and using $E = \frac{1}{2} f (r - r_{eq})^2$ then the pattern of the allowed vibration energy levels are found to be

$$E_v = (v + \frac{1}{2})\hat{w}_e - (v + \frac{1}{2})^2 w_e x_e \quad \text{cm}^{-1} \quad v=0,1,2,\dots \quad (15)$$

Where w_e is an oscillating frequency and \hat{w}_e is the oscillation frequency in wave number. X_e is the corresponding an-harmonicity constant which is positive and small for bond stretching $\approx (+0.01)$ this means that the vibration levels crowded more closely with increasing v (Banwell, C. N 1972).

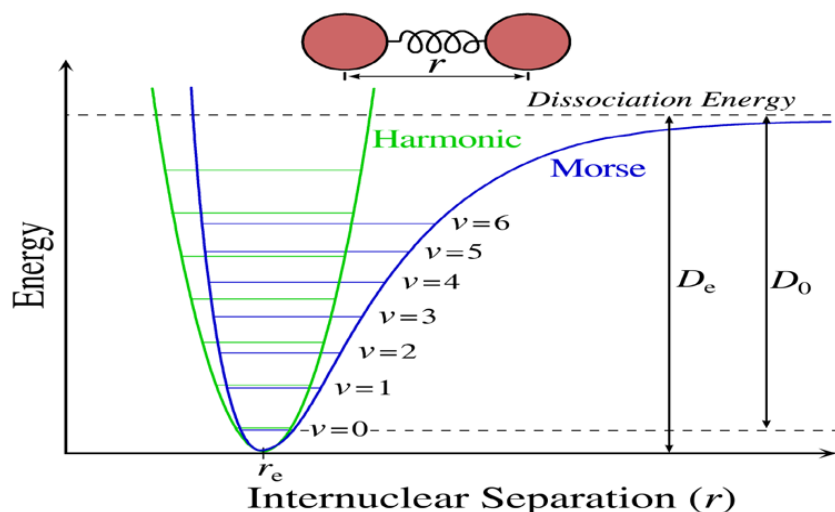


Figure 2.5: potential energy of a diatomic molecule as a function of atomic displacement (inter-nuclear separation) during vibration. The Morse potential (blue) and harmonic oscillator potential (green) (Morse, P. M. 1929; Wikipedia: Vibronic spectroscopy).

2.3 Spectroscopy

Spectroscopy is experimental techniques deal with absorption, emission, or scattering of electromagnetic radiation by atoms or molecules, it deals with interaction between EM radiation and matter (Hollas, J. 2004).

An incident photon that can induce transition between rotational levels of a molecule is found in the microwave region, while the transition between vibrational levels is induced by a photon in the infrared region, electronic transitions in atoms or molecules give radiation in the visible and UV (Ultraviolet) region (Sharma, B.K. 2007).

2.3.1. Infrared spectroscopy:

Infrared spectroscopy is a technique based on the absorption of infrared radiation by molecules, when molecules absorb infrared radiation they will be excited to a higher vibrational energy states. This absorption of infrared radiation process is quantized as a molecule absorbs only selected frequencies of infrared radiation (Pavis, D. et al 2008).

Sometimes radiation have a frequency that matches the natural vibrational frequencies of the bonds in the molecule but the bonds are not capable of absorbing it, the reason is that for bonds to be capable of absorbing infrared radiation it must possess a dipole moment that changes as a function of time at the same frequency as the incoming radiation, an example of infrared inactive molecule is homo-nuclear diatomic molecule because it's dipole moment remain zero (Stuart, B. 2004, Rosman, B. 2008).

Infrared radiation is an electromagnetic radiation lies between visible light and microwave region. It is divided into three sub regions, near, far, and mid infrared region.

Near infrared region is assumed to lie between (0.78 - 3 μm) or (12820 – 4000 cm^{-1}), mid infrared region lies between (3-30 μm) or (4000-400 cm^{-1}), and far infrared region between (30-300 μm) or (400 - 33 cm^{-1}) (Griffith, P. & Haseth, J. 2007).

The presence of hydrogen bonding is of great importance in infrared spectroscopy, it is defined as the attraction that occurs between a highly electronegative atom carrying a non-bonded electron pair (such as fluorine, oxygen or nitrogen) and a hydrogen atom, itself bonded to a small highly electronegative atom as shown in (Fig 2.6).

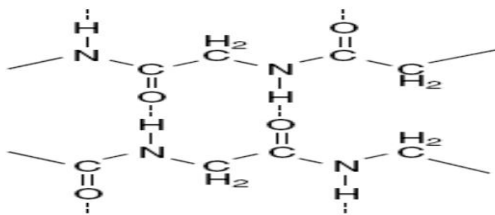


Figure 2.6: Intermolecular hydrogen bonding in a protein (dashed line).

The hydrogen bonding influences the bond stiffness and so alters the frequency of vibration. For example, for a hydrogen bond in an alcohol, the O–H stretching vibration in a hydrogen bonded dimer is observed in the 3500–2500 cm^{-1} range, rather than in the usual 3700–3600 cm^{-1} range as shown in (Fig 2.7), (Stuart, B. 2004, Griffith, P. & Haseth, J. 2007).

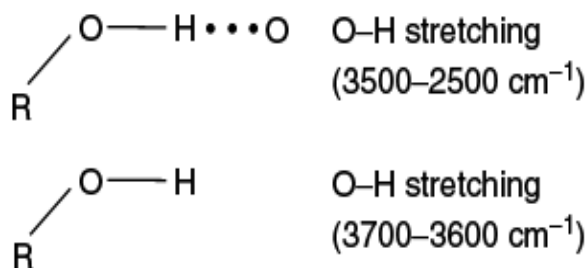


Figure 2.7: Effect of hydrogen bonding on an O–H stretching vibration (Stuart, B. 2004).

2.3.2. Fourier transforms infrared spectroscopy (FTIR):

When a sample is exposed to infrared radiation some of this radiation will be absorbed and some will pass through the sample (transmitted). The resulting spectrum shows the molecular absorption or transmission and creates a molecular fingerprint of the sample as shown in (Fig 2.8). No two molecular structures produce the same spectrum, and this make FTIR useful in studying several types of molecules (Aruldas, G. 2007; Griffith, P. & Haseth, J. 2007).

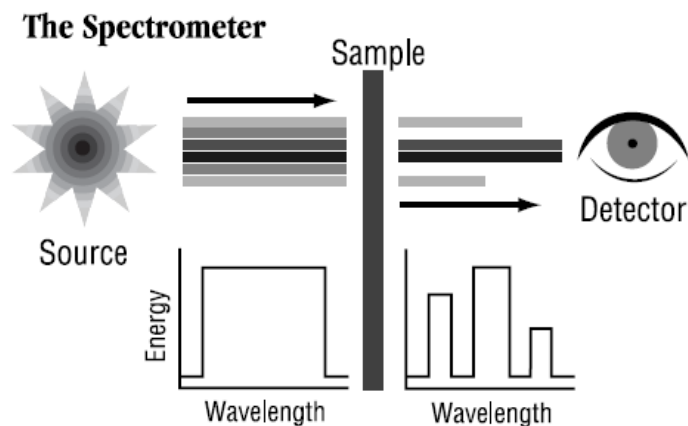


Figure 2.8: Incident and transmitted IR-radiation upon passing through a sample.

Organic molecules can absorb IR radiation between 4000 cm^{-1} and 400 cm^{-1} which corresponds to absorption of energy between 1.24meV-1.7eV. This amount of energy initiates transitions between vibrational states of bonds contained within the molecule (Buxbaum, E. 2011).

Transitions between vibrational energy levels follow the same equation as for a classical harmonic oscillator:

$$\tilde{\nu} = \frac{1}{2\pi c} \sqrt{\frac{\kappa}{\mu}} \quad (16)$$

Where $\tilde{\nu}$: is wave number in cm^{-1}

κ : is the force constant.

μ : is the reduced mass of the system, which is given by:

$$\mu = \frac{m_1 m_2}{m_1 + m_2} \quad (17)$$

From the above equations it can be noticed that as the value of force constant (k) increases the vibrational frequency and so the energy will increase, and energy will decrease when the masses increase.

The design of optical pathway produce a pattern called interferogram , FTIR uses an interferometer to process the energy that passes through the sample. In the interferometer the infrared source energy passes through a beam splitter; a mirror placed at angel 45° to the incoming radiation; that divides the beam into two perpendicular beams. As shown in the schematic diagram in (Fig.2.9). The deflected beam goes to a fixed mirror and is then returned to the beam splitter. The un-deflected light beam goes to a movable mirror and return back to the beam splitter, the path length of the second beam varies as a result of mirror motion. The two beams then recombine when they meet at the beam splitter forming a destructive or constructive interference as a result of path length difference between the two beams, and so the merged beams will cover a wide range of wavelengths. For a single IR frequency, when the two arms of the interferometer are of equal length, the two split beams travel through the exact same path length and are totally in phase with each other, thus they interfere constructively and lead to a maximum in the detector response. This position of the moving mirror is called the point of zero path difference (ZPD). When the moving mirror travels in either direction by the distance $(\lambda/4)$, the optical path (beamsplitter– mirror–beamsplitter) is changed by $2(\lambda/4)$, or $(\lambda/2)$. The two beams are 180° out of phase with each other, and thus interfere destructively. As the moving mirror travels another $(\lambda/4)$, the optical path difference is now $2(\lambda/2)$, or (λ) . The two beams are again in phase with each other and result in another constructive interference. When the mirror is moved at a constant velocity, the intensity of radiation reaching the detector varies in a sinusoidal manner to produce the interferogram output, the interferogram is a record of the interference signal, and it is a time domain spectrum (a plot of intensity of radiation versus time). Then a mathematical operation “Fourier Transform” will convert the interferogram to the final IR spectrum which is a frequency domain that is a plot of intensity versus frequency (Aruldas, G. 2007; Griffith, P. & Haseth, J. 2007; Rosman, B. 2008).

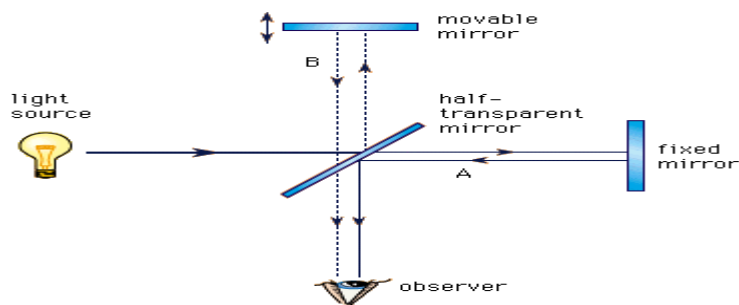


Figure 2.9: Michelson interferometer (scienceworld.wolfram.com).

The Fourier transform pairs are mathematical relations used in transformation from time domain spectrum (the changes in the radiant power $f(t)$ is recorded as a function of t) into frequency domain spectrum (which records the radiant power $G(\omega)$ a function of t) and vice versa, these two equations are:

$$G(\omega) = \frac{1}{\sqrt{2\pi}} \int_{-\infty}^{\infty} f(t) e^{i\omega t} dt \quad (18)$$

$$f(t) = \frac{1}{\sqrt{2\pi}} \int_{-\infty}^{\infty} G(\omega) e^{-i\omega t} d\omega \quad (19)$$

Where ω is the natural angular frequency (Stuart, B. 2004; G. Aruldas, G. 2007).

The transformed interferogram is then oriented toward the sample, the sample absorbs all the frequencies that match its natural vibrations. The remaining spectrum then reaches the detector (Pavis, D. et al 2008; Smith, B.C. 2011). The layout and components of FTIR are shown in (Fig 2.10).

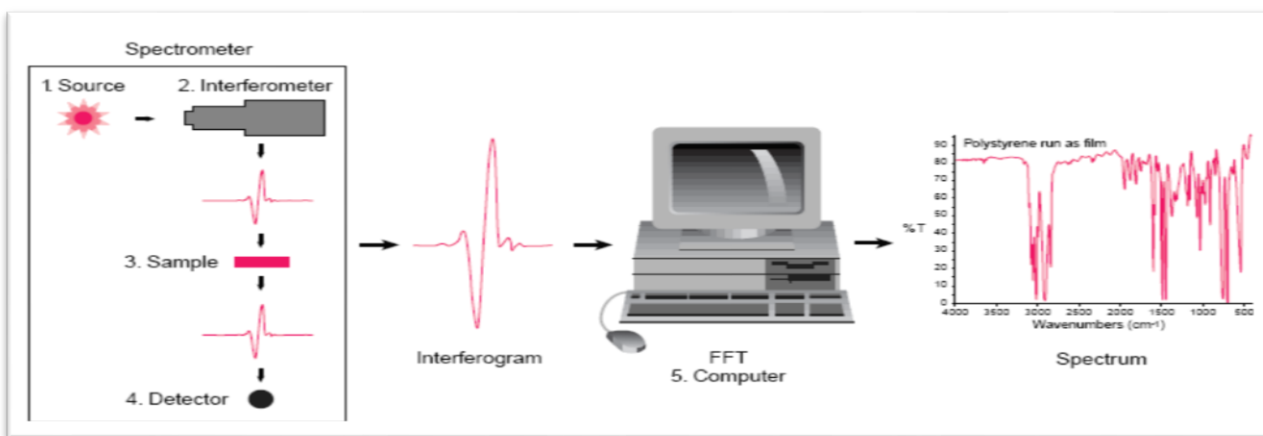


Figure 2.10: the layout and the main components of FTIR.

2.3.2.1 Amide bands:

There are nine infrared absorption bands for a polypeptide or a protein which are: amide A, B, and I-VII. The amide I and II bands are the two most prominent vibrational bands of the protein backbone. The most sensitive spectral region for the protein secondary structure is the amide I band (1700-1600 cm^{-1}), which is due almost entirely to the C=O stretching vibrations. The amide II is mainly from the in-plane NH bending vibration and from CN stretching vibrations. Other amide vibrational bands are very complex depending on the details of the force field, the nature of side chains, and hydrogen bonding. So it is rarely used in the studying of protein structure. All characteristic amide bands are shown in (Table 2.2) (Kong, J., & Yu, S. 2007; Smith, B.C. 2011; Rosman, B. 2008).

Table 2.2: Characteristic amide bands of peptide linkage (Kong, J., & Yu, S. 2007, Smith, B.C. 2011).

Nomenclature (amide)	Approximate frequency (cm^{-1})	Vibrational modes
A	~3300	NH stretching in resonance
B	~3100	with 1st amide II overtone
I	1610–1695	CO stretching
II	1480–1575	NH bending and CN stretching
III	1220–1320	CN stretching and NH bending
IV	625–765	OCN bending, mixed with other modes
V	640–800	Out-of-plane NH bending
VI	535–605	Out-of-plane CO bending
VII	~200	Skeletal torsion

In amide I region (1700-1600 cm^{-1}), molecular geometry and hydrogen bonding pattern will give rise to different C=O stretching vibration. The amide I band contour consists of overlapping component bands (α -helix, parallel β -pleated sheet, anti-parallel β -pleated sheet, random coils, and β -turns). characteristic software is used to assign each component band (Kong, J., & Yu, S. 2007).

Deuterium oxide (D_2O) is employed in infrared studies more than water (H_2O) since water absorbs strongly in the spectral region that overlap with amide I band and therefore it can affect the spectra, on the other hand D_2O has relatively low absorbance in the region between 1400-1800 cm^{-1} (Bai, Y., & Nussinov, R. 2007).

Some proteins frequencies and the assigned secondary structural element in amide I band when employing H_2O or D_2O are shown in (Table 2.3)

Table 2.3: Deconvoluted amide I band frequencies and assignments to secondary structure for protein in D2O and H2O media (Kong, J., & Yu, S. 2007).

H₂O^a		D₂O^b	
Mean frequencies	Assignment	Mean frequencies	Assignment
1,624 ± 1.0	β-sheet	1,624 ± 4.0	β-sheet
1,627 ± 2.0	β-sheet	1,631 ± 3.0	β-sheet
1,633 ± 2.0	β-sheet	1,637 ± 3.0	β-sheet
1,638 ± 2.0	β-sheet	1,641 ± 2.0	3 ₁₀ -helix
1,642 ± 1.0	β-sheet	1,645 ± 4.0	Random
1,648 ± 2.0	Random	1,653 ± 4.0	α-helix
1,656 ± 2.0	α-helix	1,663 ± 4.0	β-turn
1,663 ± 3.0	3 ₁₀ -helix	1,671 ± 3.0	β-turn
1,667 ± 1.0	β-turn	1,675 ± 5.0	β-sheet
1,675 ± 1.0	β-turn	1,683 ± 2.0	β-turn
1,680 ± 2.0	β-turn	1,689 ± 2.0	β-turn
1,685 ± 2.0	β-turn	1,694 ± 2.0	β-turn
1,691 ± 2.0	β-sheet		
1,696 ± 2.0	β-sheet		

2.3.3. Ultraviolet-Visible Spectroscopy (UV-vis):

UV-Vis spectrum results from interaction between electromagnetic radiation in the UV-Vis region and molecules, the absorption of radiation in this region depends on the electronic structure of the absorbing species, when the incident photon energy matches the difference in the energy of these electronic levels (Sharma, B.K. 2007).

To obtain UV-Vis Spectrum the sample is irradiated with electromagnetic radiation varied over a range of wavelengths in the UV or visible regions. A monochromatic radiation is employed at a time; the intensity of radiation absorbed at each wavelength is plotted against wavelength to obtain the spectrum.

The characteristics of UV-Vis spectrum depend on the structure and concentration of the absorbing species in solution (Kalsi, P.S. 2004).

The wavelength of the radiation that will be absorbed by organic molecule is determined by the difference in energy between ground state and the various excited electronic states of the molecule. Atoms in organic molecules are bonded through σ and π bonds, and the possible transitions between them is shown in (Fig. 2.11), as a rule the transition occur from HOMO (Highest Occupied Molecular Orbital) to LUMO (Lowest Unoccupied Molecular Orbital). Of all the six transitions shown in (Fig 2.11), only the two of lowest energy ($n \rightarrow \pi^*$ and $\pi \rightarrow \pi^*$) can be achieved with radiation available in the range 200-650 nm which corresponds to UV-vis region (Yadav, L.D. 2005, Kalsi, P.S. 2004; Raaman, N. 2006).

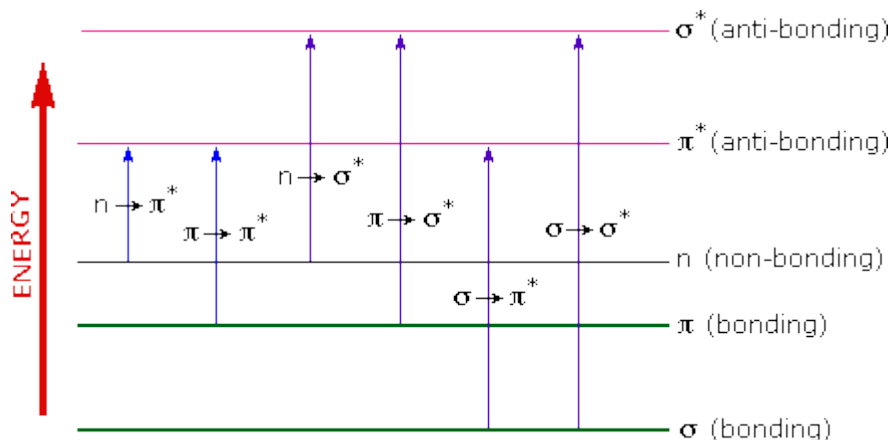


Figure 2.11: Generalized molecular orbital energy level diagram and possible transitions for organic compounds (Yadav, L.D. 2005, Raaman, N. 2006).

The $\pi \rightarrow \pi^*$ transitions are generally intense while $n \rightarrow \pi^*$ transitions are weak, so only molecules that have π bonds and atoms with non-bonding electrons absorb light in the range 200-700nm and it is called chromophores. A list of some chromopheric bonds and their absorption characteristics are given in (Table 2.4), and absorption ranges for various electronic transitions are shown in (Fig 2.12) (Kalsi, P.S. 2004).

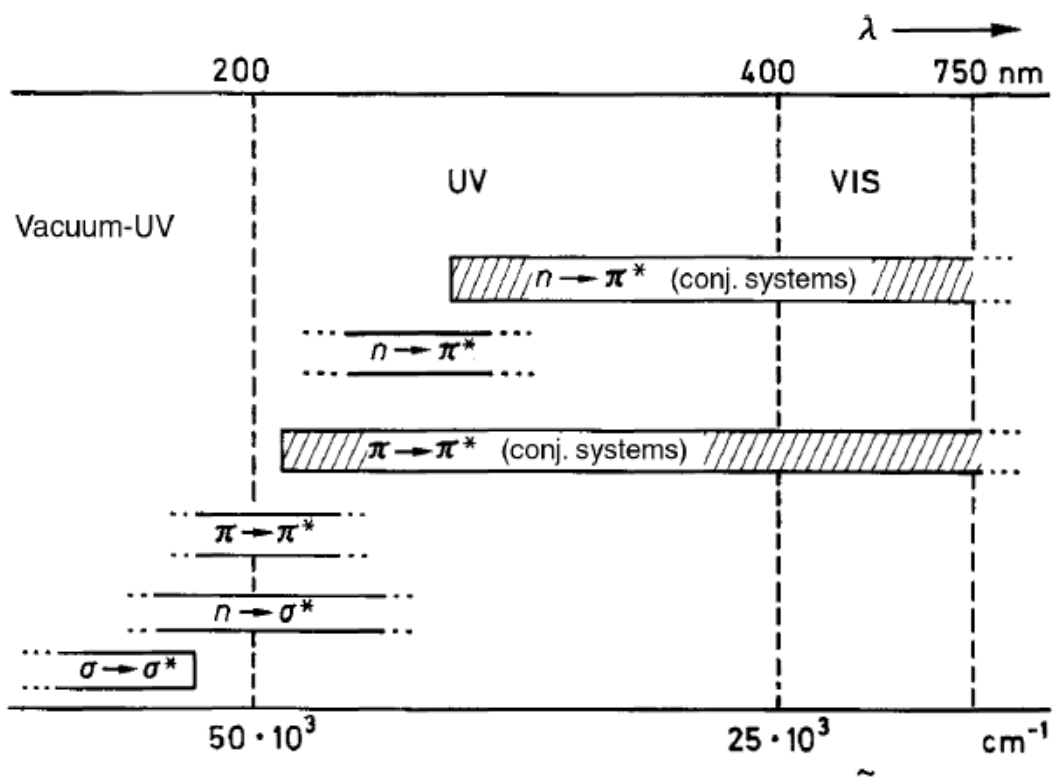
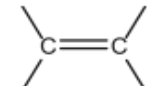
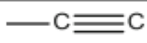
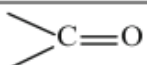
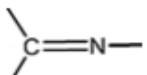


Figure 2.12: Absorption ranges for various electronic transitions.

Table 2.4: Absorption characteristics of some common chromophoric groups (Kalsi, P.S., 2004).

Chromophore	Example	λ_{\max}	ϵ_{\max}	Transition	Solvent
	Ethylene	171	15,530	$\pi \rightarrow \pi^*$	Vapor
	Acetylene	150 173	~ 10,000 6000	$\pi \rightarrow \pi^*$ $\pi \rightarrow \pi^*$	Hexane Vapor
	Acetaldehyde	160 180 290	20,000 10,000 17	$n \rightarrow \sigma^*$ $\pi \rightarrow \pi^*$ $n \rightarrow \pi^*$	Vapor Vapor Hexane
	Acetone	166 188 279	16,000 900 15	$n \rightarrow \sigma^*$ $\pi \rightarrow \pi^*$ $n \rightarrow \pi^*$	Vapor Hexane Hexane
	Acetic acid	204	60	$n \rightarrow \pi^*$	Water
	Acetamide	178 220	9500 63	$\pi \rightarrow \pi^*$ $n \rightarrow \pi^*$	Hexane Water
	Ethyl acetate	211	57	$n \rightarrow \pi^*$	Ethanol
	Nitromethane	201 274	5000 17	$\pi \rightarrow \pi^*$ $n \rightarrow \pi^*$	Methanol Methanol
	Acetoxime	190	5000	$n \rightarrow \pi^*$	Water
	Acetonitrile	167	Weak	$\pi \rightarrow \pi^*$	Vapor
	Azomethane	338	4	$n \rightarrow \pi^*$	Ethanol

2.3.4 Fluorescence:

Luminescence is the emission of light from atoms when it is electronically excited. It is divided into two categories fluorescence and phosphorescence.

At room temperature most of the electrons occupy the lowest vibrational level of the ground electronic state (S_0), and when they absorb light they produce excited states, the transitions to the first and the second excited states (S_1 , S_2 respectively) are shown in (Fig. 2.13) (Schulman, S.G. 1977).

When a molecule absorbs energy, it reaches a higher vibrational level of the excited state, if it maintains its spin, it is a singlet state (S) while if its spin is changed it is a triplet state (T), the excited molecule then rapidly loses its excess of vibrational energy and falls to the lowest vibrational level of the excited state. Returning from singlet state to the ground state is fast while returning from triplet state requires spin reversal and so is slower and less likely to occur. As shown in (Fig. 2.13) there are sub states associated with each singlet or triplet states they are caused by vibration and rotation of the molecule.

If the energy of the sub-states of the ground state and those of the excited state overlap, direct return of the electron to the ground state is possible by internal conversion, the energy difference is converted to molecular vibration, that is, heat. If the energy of the sub-states of the ground state and those of the excited state do not overlap, then direct returning to the ground state is impossible, instead the electron first falls to S_1 via internal conversion, and from there it returns to S_0 by emission of light as shown in (Fig. 2.13), the energy difference between S_2 and S_1 is lost as molecular vibration (heat), and thus the light emitted will have less energy and so longer wave length than that absorbed this phenomena is called fluorescence (Lakowicz, J.R. 2002; Sharma, B.K. 2007; Buxbaum, E. 2011). Fluorescence usually occurs from fluorescent substances such as aromatic molecules called fluorophores. Fluorophores are divided into two main classes: intrinsic fluorophores which occur naturally such as amino acids (aromatic amino acids Tryptophan, tyrosine, and phenylalanine), and extrinsic fluorophores which are added to the sample to provide fluorescence when it does not exist or to change the spectral properties of the sample (Lakowicz, J.R., 2006).

2.3.5. Fluorescence Quenching:

Fluorescence quenching can be defined as a bimolecular process that reduces the fluorescence intensity without changing the fluorescence emission spectrum; it can result from transient excited-state interactions (collisional quenching) or from formation of non-fluorescent ground-state species.

For collisional quenching the decrease in intensity is described by the well-known Stern-Volmer equation:

$$\frac{F_0}{F} = 1 + K_q \tau_0 [L] \quad (20)$$

Where: K is the Stern-Volmer quenching constant, k_q is the bimolecular quenching constant, τ is the unquenched lifetime, and $[L]$ is the quencher concentration.

The Stern-Volmer quenching constant K indicates the sensitivity of the fluorophore to a quencher. A fluorophore buried in a macromolecule is usually inaccessible to water soluble quenchers, so that the value of K is low. Larger values of K are found if the fluorophore is free in solution or on the surface of a biomolecule.

Fluorescence spectroscopy can be applied to a wide range of problems in the chemical and biological sciences. The measurements can provide information on a wide range of molecular processes, including the interactions of solvent molecules with fluorophores, conformational changes, and binding interactions (Lakowicz, J.R., 2006).

The fluorescence of HSA results from the tryptophan, tyrosine, and phenylalanine residues. The intrinsic fluorescence of many proteins is mainly contributed by tryptophan alone, because phenylalanine has very low quantum yield and the fluorescence of tyrosine is almost totally quenched if it is ionized or near an amino group, a carboxyl group, or a tryptophan residue (Darwish, S. M., et al. 2010). The maximum value for the dynamic bimolecular quenching

constant is $(2.0 \times 10^{10} \text{ M}^{-1} \text{ s}^{-1})$ (Litwack. G, & Axelord. J. 1970), and the fluorescence life time is about 10^{-8} s, so if the quenching constant is larger than the maximum value so the quenching is static and the equation which is used is:

$$\frac{1}{F_0 - F} = \frac{1}{F_0 K(L)} + \frac{1}{F_0} \quad (21)$$

Where K is the binding constant of Retinol (Vitamin A₁) with HSA. When we plot $1/(F_0 - F)$ Vs. $1/L$ we can find the value of the binding constant from the slope and the intercept (Brandt 1999).

2.4 Proteins

Proteins are important organic chemical substances in our life and the major target of many types of medication in our body (Zhang, G., et al. 2008). Proteins are a particular type of biological molecules that can be found in every single living being on Earth. Proteins: are polymers consisting of amino acids linked by peptide bonds. Proteins perform a vast array of functions within living organisms, including catalyzing metabolic reactions, replicating DNA, responding to organisms, and transporting molecules from one location to another (Nelson DL, & Cox MM 2005).

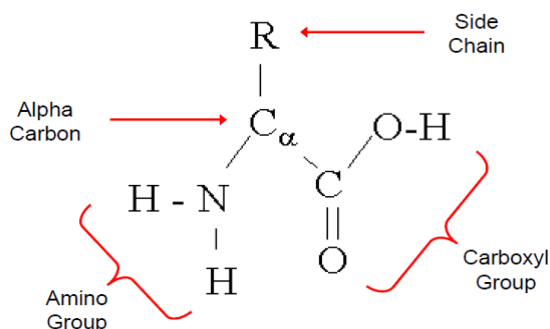


Figure 2.13: Amino acid structure (Nelson DL, & Cox MM 2005).

Each amino acid consists of a central carbon atom (alpha-carbon), an amino group (NH₂), and a carboxyl group (COOH) and a side chain. The differences in side chains distinguish different amino acids from each other (Colin, D. 2014).

2.4.1 Protein Structure

Protein chemical structure and molecular conformation are commonly described in terms of four levels of structure: Primary structure, Secondly structure, Tertiary structure and Quaternary structure.

1. Primary structure refers to a linear sequence of amino acids. It is sometimes called the "covalent structure" of proteins because most of the covalent bonding within proteins defines the primary structure (Gorga, F.R. 2007).

2. The secondary structure is the result of hydrogen bonds between the repeating constituents of the polypeptide backbone (not the amino acid side chains). Within the backbone, the oxygen atoms have a partial negative charge, and the hydrogen atoms attached to the nitrogen have a partial positive charge. Therefore, hydrogen bonds can form between these atoms. Individually, these hydrogen bonds are weak, but because they are repeated many times over a relatively long region of the polypeptide chain, they can support a particular shape for that part of the protein (Reece, J. B., et al 2011).

The two most common secondary structure elements are alpha helices and beta sheets see figure (2.14) .

Alpha Helix is the most common structural motif found in proteins; in globular proteins over 30 percent of all residues are found in helices (Whitford, D. 2005). It is a cylindrical shape formed by a coiling of the polypeptide chain on itself with interactions take place between group's 3-4 amino acid residues apart. (Hydrogen bonds between the hydrogen atoms attached to the amide nitrogen and the carbonyl oxygen atom). The first four NH groups and last four CO groups will normally lack backbone hydrogen bonds (Gropper, S. S., et al. 2009).

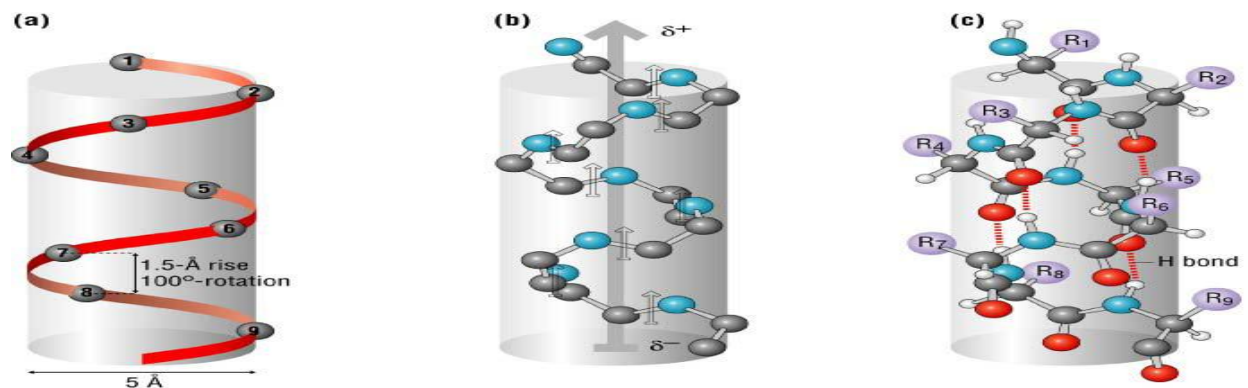


Figure 2.14: Alpha Helix Protein (Gropper, S. S., et al. 2009).

Beta Pleated Sheet: in this structure, the polypeptide chain is fully stretched out with the side chains positioned either up or down. The stretched polypeptide can fold back on itself with its segments packed together (Gropper, S. S., et al 2009).

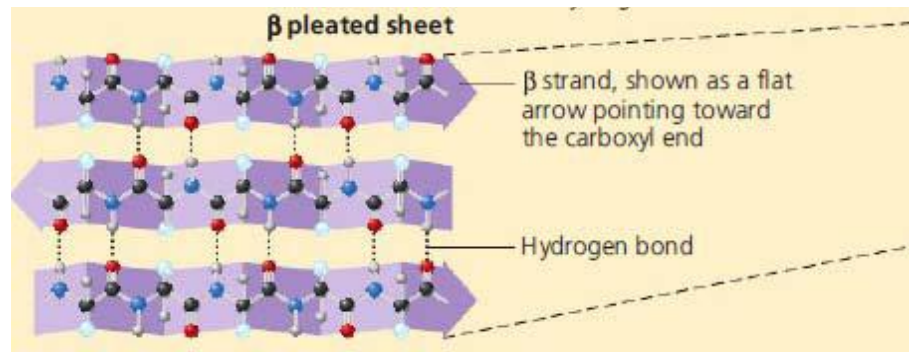


Figure 2.15: Beta Pleated Sheet (Gropper, S. S., et al 2009).

β strands can interact in either parallel or anti-parallel orientation, and each of the two forms has a distinctive pattern of hydrogen bonding. Figures (2.16 & 2.17) illustrate examples of anti-parallel and parallel β sheets from real protein structures.

The anti-parallel sheet has hydrogen bonds perpendicular to the strands, and narrowly spaced bond pairs alternate with widely spaced pairs. Looking from the N- to C-terminal direction along the strand, when the side chain points up the narrow pair of H bonds will point to the right. Parallel sheet has evenly spaced hydrogen bonds (Richardson, J.S. 2007).

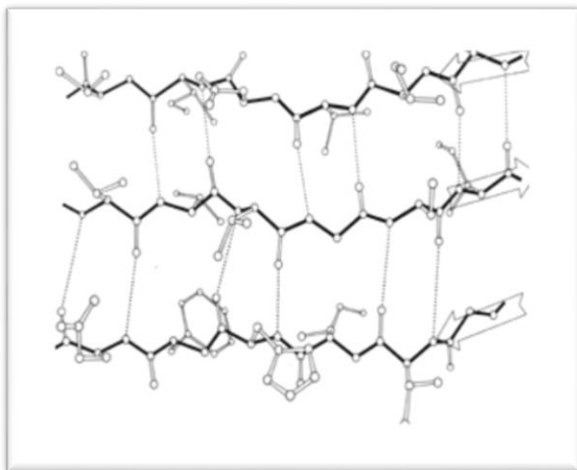


Figure 2.16: Anti parallel Beta Pleated Sheet Protein (Richardson, J.S. 2007).

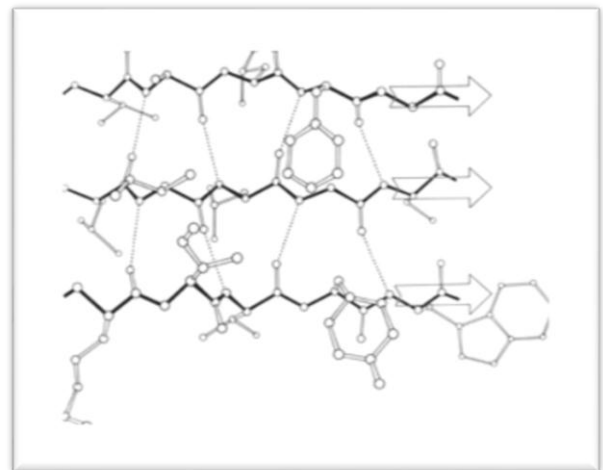


Figure 2.17: Parallel Beta Pleated Sheet Protein (Richardson, J.S. 2007).

There are other secondary structure elements such as turns, coils, 3_{10} helices etc.

Tertiary structure describes the way in which the elements of protein secondary structure are arranged in space and Quaternary structure describes how several polypeptide chains come together to form a single functional protein (Cooper, A. 2004).

2.5 Human Serum Albumin (HSA).

Human serum albumin HSA is an abundant plasma protein that binds a wide variety of hydrophobic ligands including fatty acids, bilirubin, thyroxin and hemin and also drugs (Carter, et al 1989). The most important physiological role for the protein is to bring such solutes into blood stream and then deliver them to the target organs, as well as to maintain the pH and osmotic pressure of plasma (Abu Teir, M., et al 2010; Abu Teir, M. M., et al 2014). HSA concentration in blood plasma is 40 mg/ml. The three dimensional structure of HSA was determined through x-ray crystallographic measurements (Carter, et al 1989). This globular protein is of Mw 65 K and consists of 585 amino acids. Its amino-acid sequence contains a total of 17 disulphide bridges, one free thiol (Cys 34), and a single tryptophan (Trp 214). The disulphide is positioned in a repeating series of nine loop-link loop structures centered on eight sequential Cys-Cys pairs. (Xiao-Min-He, et al 1992)

It became evident from early heavy-atom derivative screens and from preliminary binding studies that the principal binding regions on HSA were located in sub-domains I, II and III each containing two subdomains (A&B) and stabilized by 17 disulfide bridges (Xiao-Min-He, et al 1992; Ouameur,A., et al 2004). Aromatic and heterocyclic ligands were found to bind within two hydrophobic pockets in sub-domains IIA and IIIA, which are site I and site II. Site I is dominated by strong hydrophobic interaction with most neutral, bulky, heterocyclic compounds, while site II mainly dipole-dipole, van de Waals, and/or hydrogen-bonding interactions with many aromatic carboxylic acids (Ouameur,A., et al 2004). HSA contained a single tryptophan residue (Trp 214) in domain IIA and its intrinsic fluorescence is sensitive to the ligands bounded nearby (Krishnakumar, S.S., et al 2002). Therefore, it is often used as a probe to investigate the binding properties of drugs with HSA.

It has been shown that the distribution free concentration and the metabolism of various drugs can be significantly altered as a result of their binding to HSA (Kang, J., et al 2004).The binding properties of albumin depend on the three dimensional structure of the binding sites, which are distributed over the molecule. Strong binding can decrease the concentrations of free drugs in plasma, whereas weak binding can lead to a short lifetime or poor distribution. Its remarkable capacity to bind a variety of drugs results in its prevailing role in drug pharmacokinetics and pharmacodynamics (Kandagal ,P.B., et al 2007). Multiple drug binding sites have been reported for HSA by several researchers (Bhattacharya, A., et al 2000).

The distribution and metabolism of many biologically active compounds in our body whether drugs or natural products are correlated with their affinities toward serum albumin which is the most abundant protein carrier in our plasma. So the study of the interaction of such molecules for example Retinol (Vitamin A₁) with albumin is of a fundamental importance. Some investigations have been applied on Retinol -HSA interaction but none of them determined in details neither Retinol -HSA binding constant (k) nor the effect of Retinol complexes on the protein structure, as what have been studied in this research. Some investigations only indicated

that the interaction occurred and others used the equilibrium dialysis method to calculate the binding constant (k) (Ouameur, A., et al 2004) (IUPAC, 1997).

2.6 Retinol (Vitamin A₁)

Vitamin A is essential throughout life as it is required in reproduction, embryonic and foetal development, vision, growth, differentiation and tissue maintenance (Sommer A. et al 2008; Bates, CJ. 1995). The term vitamin A covers the retinoids, a group of lipid-soluble compounds which have similar physiological functions and metabolic activities: retinol, retinal (the aldehyde form), and retinoic acid. Retinol inter-converts between retinyl esters and retinal, while retinoic acid (which is not found in the diet) is an end product of retinol conversion. These substances have different actions: retinoic acid is required for the growth and differentiation of epithelial cells, whereas retinyl ester, retinol and retinal can all support cellular differentiation, reproduction and visual functions. Retinoic acid is the form of vitamin A for which a teratogenic effect on the foetus has been demonstrated and which acts as a hormone in many cells by regulating gene expression, thus controlling cell differentiation and maturation (lammer EJ, et al 1985).

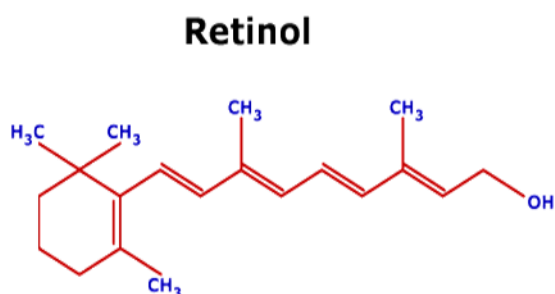


Figure 2.18: Chemical structure of Retinol (vitamin A₁) (Wikipedia: Retinol).

Vitamin A nutrition is quite complex and needs to be considered in terms of its relationship with other vitamins. For example, vitamin A works cooperatively at the genetic level with vitamin D. Vitamin E is required for the conversion of β -carotene to retinol (see below), while vitamin A absorption can be reduced by excess vitamin E consumption. In turn, excess dietary vitamin A can interfere with vitamin K absorption. The conclusion is that although supplementation with vitamin A may be appropriate in cases of proven deficiency, a vitamin-rich mixed diet is the best way to maintain optimum vitamin A status (Bates, CJ. 1995; Sommer A. et al, 2008).

Chapter Three

Experimental Part

Chapter Three

Experimental part.

This chapter consists of three sections; section one deal with samples, and film preparation. Section two describes the spectrometers used in this work, which is UV-VIS spectrophotometer (Nano Drop ND-1000), and Fluorospectrometer (NanoDrop ND-3300), and Bruker IFS 66/S FT-IR . The final section presents the experimental procedure in details.

3.1 Samples and materials.

HSA (fatty acid free), Retinol (Vitamin A₁) were purchased from Sigma Aldrich chemical company and used without further purifications. The data were collected using samples in the form of thin films for FT-IR measurements and liquid form for UV-VIS. Preparations of the thin film samples required three stock solutions as described below:

3.1.1 Preparation of HSA stock solution:

HSA was dissolved in 25% ethanol in phosphate buffer Saline and at physiological (pH 6.9- 7.4), to a concentration of (80mg/ml), and used at final concentration of (40 mg/ml) in the final Retinol - HSA solution.

3.1.2 Preparation of Retinol (Vitamin A₁) stock solution:

Retinol (Vitamin A₁) with molecular weight of (286.459 g/mol), was dissolved in 25% ethanol in phosphate buffer Saline and, then the solution was placed in ultrasonic water path (SIBATA AU-3T) for two days to ensure that all the amount of Retinol was completely dissolved.

3.1.3 HSA- Retinol (Vitamin A₁) samples:

HSA concentration was fixed at 40 mg.ml⁻¹ in all samples. However, the concentration of retinol in the final HSA- Retinol solutions was decreased such that the molecular ratios (HSA: retinol) are 1:20, 1:10, 1:5, 1:2, and 1:1. All samples were made by mixing equal volume from HSA to equal volume from different concentration of retinol.

3.1.4 Thin film preparations:

Silicon windows (NICODOM Ltd) were used as spectroscopic cell windows. The optical transmission is high with little or no distortion of the transmitted signal. The 100% line of a NICODOM silicon window shows that the silicon bands in the mid- IR region do not exhibit total absorption and can be easily subtracted. 40 µl of each sample of HSA – Retinol was spread on a silicon widow and an incubator was used to evaporate the solvent, to obtain a transparent thin film on the silicon window. All solutions were prepared at the same time for one run at room temperature 25⁰c. The same procedure was followed for HSA- retinol films preparation.

3.2 Instruments

Two instruments were used in studying the interaction of HSA with retinol. In this work the following instruments have been used in taking the measurements:

3.2.1 FT-IR Spectrometer:

The FT-IR measurements were obtained on a Bruker IFS 66/S spectrophotometer equipped with a liquid nitrogen-cooled MCT detector and a KBr beam splitter. The spectrometer was continuously purged with dry air during the measurements.

3.2.2 UV-VIS spectrophotometer (Nano Drop ND-1000):

The absorption spectra were obtained by the use of a Nano Drop ND-1000 spectrophotometer. It is used to measure the absorption spectrum of the samples in the range between 220-750nm, with high accuracy and reproducibility.

3.2.3 Fluorospectrometer (Nano Drop 3300):

The fluorescence measurements were performed by a Nano Drop ND-3300 Fluorospectrophotometer at 25°C. the excitation source comes from one of three solid-state light emitting diodes (LED's). The excitation source options include: UV LED with maximum excitation 365 nm, Blue LED with excitation 470 nm, and white LED from 500 to 650nm excitation. A 2048-element CCD array detector covering 400-750 nm, is connected by an optical fiber to the optical measurement surface. The excitation is done at the wavelength of 360 nm and the maximum emission wavelength is at 439 nm. Other equipment such as Digital balance, pH meter, Vortex, Plate stir...and Micropipettes were used (Nano Drop 3300 Fluorospectrometer V2.7 user's Manual 2008).

3.3 Experimental procedures

3.3.1 UV-VIS Spectrophotometer experimental procedures:

Procedure of UV-VIS spectrophotometer was followed as described in Nano Drop 1000 Spectrophotometer V3.7, 2008, User's Manual (Nano Drop 1000 Spectrophotometer V3.7, User's Manual, 2008).

Basic Use: The main steps for using the sample retention system are listed below:

1. With the sampling arm open, pipette the sample onto the lower measurement pedestal.
2. Close the sampling arm and initiate a spectral measurement using the operating software on the PC. The sample column is automatically drawn between the upper and lower measurement pedestals and the spectral measurement made.

3. When the measurement is complete, open the sampling arm and wipe the sample from both the upper and lower pedestals using a soft laboratory wipe. Simple wiping prevents sample carry over in successive measurements for samples varying by more than 1000 fold in concentration.

3.3.2 Fluorospectrometer experimental procedures:

Procedure of Fluorospectrophotometer was followed as described in Nano Drop 3300 Fluorospectrometer V2.7,2008 User's Manual, (Nano Drop 3300 Fluorospectrometer V2.7 User's Manual, 2008), which is as follows: Before taking the measurements of samples the Nano Drop 3300 Fluorospectrometer was "blanked". Operation A 2.5 μ l sample of Retinol is pipetted onto the end of the lower measurement pedestal (the receiving fiber). A non-reflective "bushing" attached to the arm is then brought into contact with the liquid sample causing the liquid to bridge the gap between it and the receiving fiber. The gap, or path-length, is controlled to 1mm. following excitation with one of the three LEDs; emitted light from the sample passing through the receiving fiber is captured by the spectrophotometer. The Nano Drop 3300 is controlled by software run from a PC. All data is logged and archived in a folder at a user defined location.

Basic Use: The main steps for making a measurement are listed below:

1. With the sampling arm open, pipette the sample into the lower measurement pedestal see no.1 of figure 3.1.
2. Close the sampling arm and initiate a measurement using the operating software on the PC. The sample column is automatically drawn between the upper bushing and the lower measurement pedestal and the measurement is made see photo no.2 of figure 3.1.
3. When the measurement is complete, open the sampling arm and wipe the sample from both the upper bushing and the lower pedestal using low lint laboratory wipe see photo no.3 of figure 3.1.



Figure 3.1: Main steps for using the sample fluorospectrophotometer (Nano Drop 3300).

3.3.3 FT-IR Spectrometer experimental procedures:

The absorption spectra were obtained in the wave number range of 400–4000 cm^{-1} . A spectrum was taken as an average of 60 scans to increase the signal to noise ratio, and the spectral resolution was at 4 cm^{-1} . The aperture used in this study was 8 mm, since we found that this aperture gives best signal to noise ratio. Baseline correction, normalization and peak areas calculations were performed for all the spectra by OPUS software. The peak positions were determined using the second derivative of the spectra. The infrared spectra of HSA, retinol – HSA complexes, were obtained in the region of 1000–1800 cm^{-1} . The FT-IR spectrum of free HSA was acquired by subtracting the absorption spectrum of the buffer solution from the spectrum of the protein solution. For the net interaction effect, the difference spectra {(protein and retinol solution) – (protein solution)} were generated using the featureless region of the protein solution 1800-2200 cm^{-1} as an internal standard (Surewicz, W., et al 1987).

3.3.3.1 FT-IR data processing:

FT-IR spectroscopy presents several advantages over conventional dispersive techniques for this type of analysis through the application of second derivative, peak picking, spectral subtraction, baseline correction, smoothing integration, curve fitting, and Fourier self-deconvolution. In the present study several data processing tasks were used, such as:

3.3.3.1 Baseline correction.

The baseline correction method applied here includes two steps. The first step is to recognize the baseline; this is done by selecting a point from spectral points on the spectrum. Then adding or subtracting intensity value from the point or points to correct the baseline offset. Baseline correction task is used to bring the minimum point to zero. This is done automatically using Optic User Software (OPUS) and successfully removes most baseline offsets (Griffith, P. & Haseth, J. 2007; OPUS Bruker manual , 2004).

3.3.3.2 Peak picking.

Automated peak picking involves two steps: (1) the recognition of peaks, and (2) the determination of the wavenumber values of maximum or minimum absorbance. A threshold absorbance value is usually set so that weak bands are not measured (Griffith, P. & Haseth, J. 2007).

3.3.3.3 Second derivative.

Increased separation of the overlapping bands can be achieved by calculating the second derivative rate of change of slope of the absorption spectrum, second-derivative procedure have been successfully applied in the qualitative study of a large number of proteins (Haris , P.I., et al 1999).

3.3.3.4 Fourier self-deconvolution.

The Fourier deconvolution procedure, sometimes referred to as ‘resolution enhancement’ is the most widely used band narrowing technique in infrared spectroscopy of biological materials (Jackson, M., et al 1991). It involves narrowing the widths of infrared bands, allowing increased separation of the overlapping components present within the broad band envelope (Kauppinen, J. K., et al 1981). Both second-derivative and deconvolution procedures have been successfully applied in the qualitative study of a large number of protein. (Workman, J., 1998; Kauppinen, J. K., et al 1981). In addition to providing valuable information about their secondary structure, the method has been shown to be useful for detecting conformational changes arising as a result of ligand binding, pH, temperature, organic solvents, detergents, ... etc. In many cases results obtained using this approach has been later supported by studies using other techniques such as X-ray diffraction and NMR. However, both derivative and deconvolution techniques should be applied with care since they amplify the noise significantly (Haris , P. I., et al 1999).

3.3.3.5 Spectral subtraction.

Difference spectroscopy is another approach that is very useful for investigating subtle differences in protein structure. The principle of difference spectroscopy involves the subtraction of a protein absorbance spectrum in state A from that of the protein in state B. The resultant difference spectrum only shows peaks that are associated with those groups involved in the conformational change (Goormaghtigh, E., et al 1990; Haris , P. I., et al 1999). The accuracy of this subtraction method is tested using several control samples with the same protein or drug concentrations, which resulted into a flat base line formation.

3.3.3.6 Curve fitting.

The Curve Fit command allows calculating single components in a system of overlapping bands. A model consisting of an estimated number of bands and a baseline should be generated before the fitting calculation is started. The model can be set up interactively on the display and is optimized during the calculation (OPUS Bruker manual, 2004).

Chapter Four

Results and Discussion

Results and Discussion

The experimental results are presented as follows: the first section deals with UV-absorption spectroscopy. The second section discusses fluorescence spectroscopy results. In the last section discusses Fourier transform infrared spectroscopy results.

4.1 UV-absorption spectroscopy

In this section, I will discuss the results of the absorption spectra of HSA- retinol mixtures at different concentrations of retinol respectively. The excitation has been done on 210 nm and the absorption is recorded at 280 nm. The UV absorbance intensity of HSA increased with the increasing of retinol concentration as shown in figure 4.1. In addition, the binding of the Retinol to HSA resulted in a slight shift of the HSA absorption spectrum. These results clearly indicate that an interaction and some complex formation occurred between HSA and retinol separately, and also indicate that the peptide strands of protein molecules extended more upon the addition of retinol to HSA (Peng, L., et al 2008; Abu Tair, M., et al 2010).

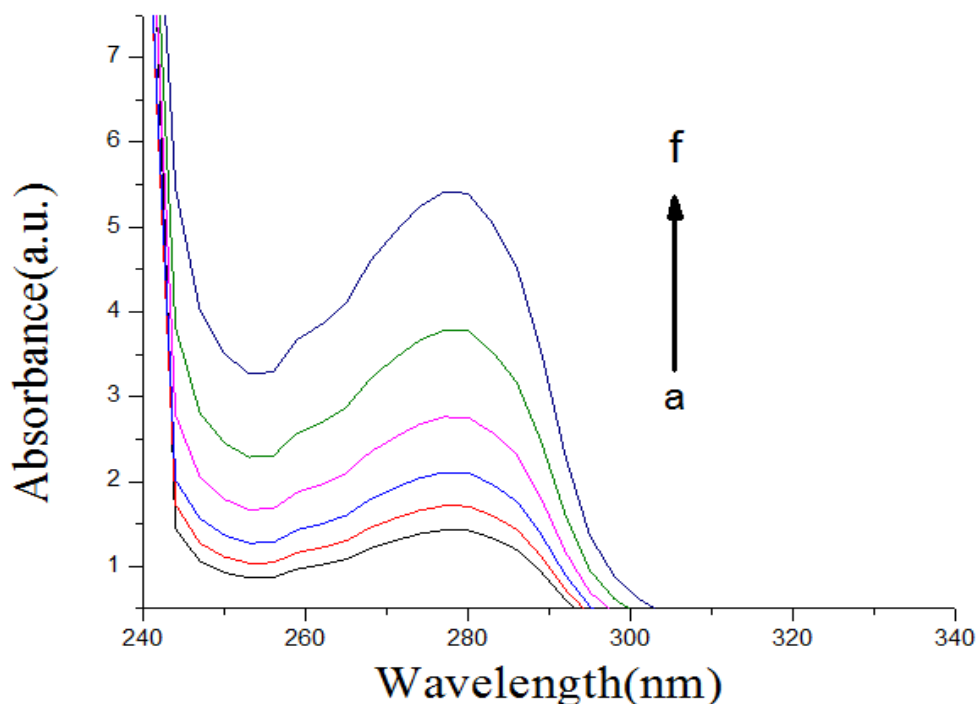


Figure 4.1: UV-Absorbance spectra of HSA with different molar ratios of retinol, HSA: retinol (a=1:0, b=1:1, c=1:2, d=1:5, e=1:10, f=1:20), no UV absorption for retinol.

4.1.1 Binding constants of retinol and HSA complexes using UV-VIS Spectrophotometer:

The retinol - HSA complexes binding constants were determined using UV-VIS spectrophotometer results according to published method (Stephanos, J., et al 1996; Klotz, M.I., et al 1971; Ouameur, A., et al., 2004), by assuming that there is only one type of interaction between retinol and HSA in aqueous solution, which leads to establish Equations. (1) and (2) as follows:



$$K = [\text{Retinol: HSA}] / [\text{Retinol}][\text{HSA}] \quad (2)$$

The absorption data were treated using linear double reciprocal plots based on the following equation (Lakowicz, J.R., 2006):

$$\frac{1}{A-A_0} = \frac{1}{A_\infty-A_0} + \frac{1}{K[A_\infty-A_0]} \times \frac{1}{L} \quad (3)$$

where A_0 corresponds to the initial absorption of protein at 280 nm in the absence of ligand, A_∞ is the final absorption of the ligated protein, and A is the recorded absorption at different Retinol concentrations (L). The double reciprocal plot of $1/(A - A_0)$ vs. $1/L$ is linear as it shown in Figure 4.3 and 4.4 and the binding constant (K) can be estimated from the ratio of the intercept to the slope to be $(1.7176 \times 10^2 \text{ M}^{-1})$ for Retinol - HSA complexes, respectively. The values obtained is indicative of a weak Retinol protein interaction with respect to the other Retinol -HSA complexes with binding constants in the range of 10^5 and 10^6 M^{-1} (Kragh- Hanse, U., 1981). The reason for the low stability of the Retinol -HSA complexes can be attributed to the presence of mainly hydrogen bonding interaction between protein and the Retinol polar groups or an indirect vitamin - protein interaction through water molecules (Sulkowaska, A., et al 2002). Similar weak interactions were observed in *cis* Pt(NH₃)₂-HSA and taxol-HSA complexes (Purcell, M., et al 2000; Neault, J.F., et al 1998).

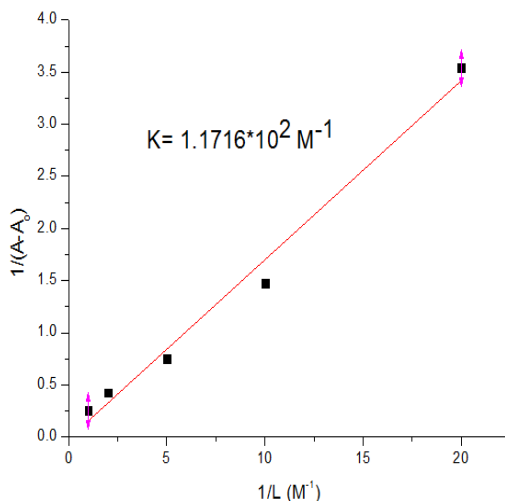


Figure 4.2: The plot of $1/(A-A_0)$ vs. $1/L$ for HSA with different concentrations of retinol

4.2 Fluorescence spectroscopy

Fluorescence spectroscopy is another technique that is used widely to study binding between protein and ligand. The Fluorescence absorbance intensity of HSA increased with the increasing of retinol concentration. Various molecular interactions can decrease the fluorescence intensity of a compound such as molecular rearrangements, excited state reactions, energy transfer, ground state complex formation, and collisional quenching (Turro, N.J. 1991; Sheehan, D. 2009). The excitation is done on 350 nm and emission occurs at 439 nm. The fluorescence emission spectra of HSA with various concentrations of Retinol (a=1:0, b=1:1, c=1:2, d=1:5, e=1:10, f=1:20) are shown in (Fig 4.3).

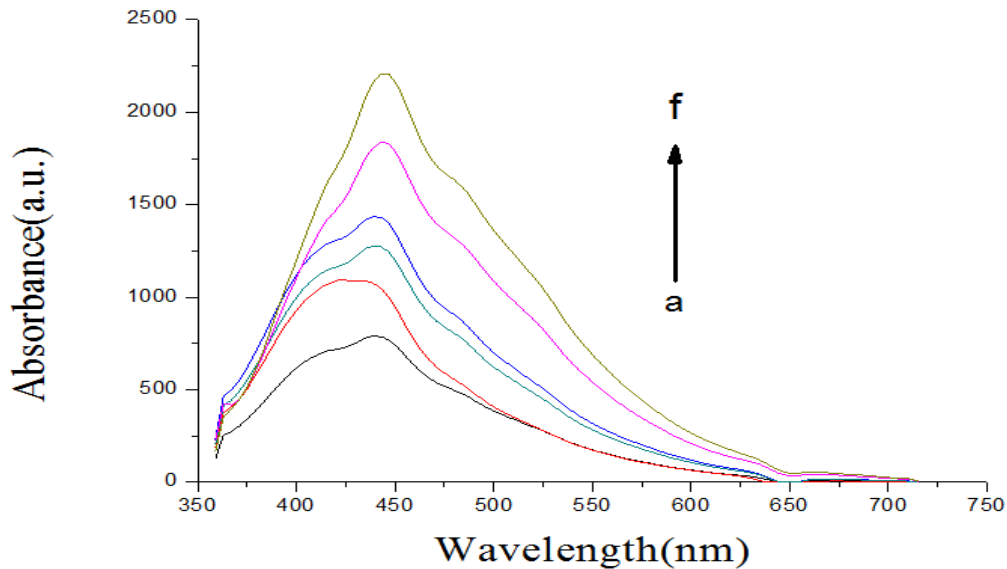


Figure 4.3: The fluorescence emission spectra of HSA with various concentrations of Retinol (a=1:0, b=1:1, c=1:2, d=1:5, e=1:10, f=1:20)

4.2.1. Determination of Stern-Volmer quenching constants (K_{sv}) and the quenching rate constant (K_q):

Fluorescence quenching can be induced by different mechanisms that were usually classified into static quenching and dynamic quenching. Dynamic quenching arises from collisional encounters between the fluorophores and quenchers while static quenching results from the formation of a ground state complex between the fluorophores and the quenchers (Turro, N.J. 1991).

For dynamic quenching, the decrease in fluorescence intensity is described by Stern-Volmer equation (Lakowicz, J.R., 2006; Sheehan, D. 2009).

$$\frac{F_0}{F} = 1 + K_{sv}[L] = 1 + K_q \tau_0 [L] \quad (4)$$

Where F and F_0 are the fluorescence intensities with and without quencher, K_q is the quenching rate constant, K_{sv} is the Stern-Volmer quenching constant, $[L]$ is the concentration of Retinol, and τ_0 is the average lifetime of the biomolecule without quencher.

The Stern-Volmer quenching constants K_{sv} were obtained by finding the slope of the linear curve obtained when plotting $\frac{F_0}{F}$ vs $[L]$. The quenching rate constant K_q can be calculated using the fluorescence lifetime of HSA to be 10^{-8} s (Cheng, F. Q., et al 2006).

The plots of $\frac{F_0}{F}$ vs $[L]$ for HSA- Retinol complexes are shown in (Fig 4.4). From these plots the Stern-Volmer quenching constants for HSA- Retinol complexes were found to be $(1.885 \cdot 10^2 \text{ M})$.

The quenching rate constants for HSA- Retinol were then calculated to be $(1.885 \cdot 10^{10} \text{ L Mol}^{-1} \text{ s}^{-1})$. The obtained values of the quenching rate constants of retinol are equal the maximum dynamic quenching constants for various quenchers with biopolymers $(2 \cdot 10^{10} \text{ L Mol}^{-1} \text{ s}^{-1})$ which confirms that static quenching is dominant in these complexes (Wang, T., et al. 2008; Darwish, S.M. et al 2012).

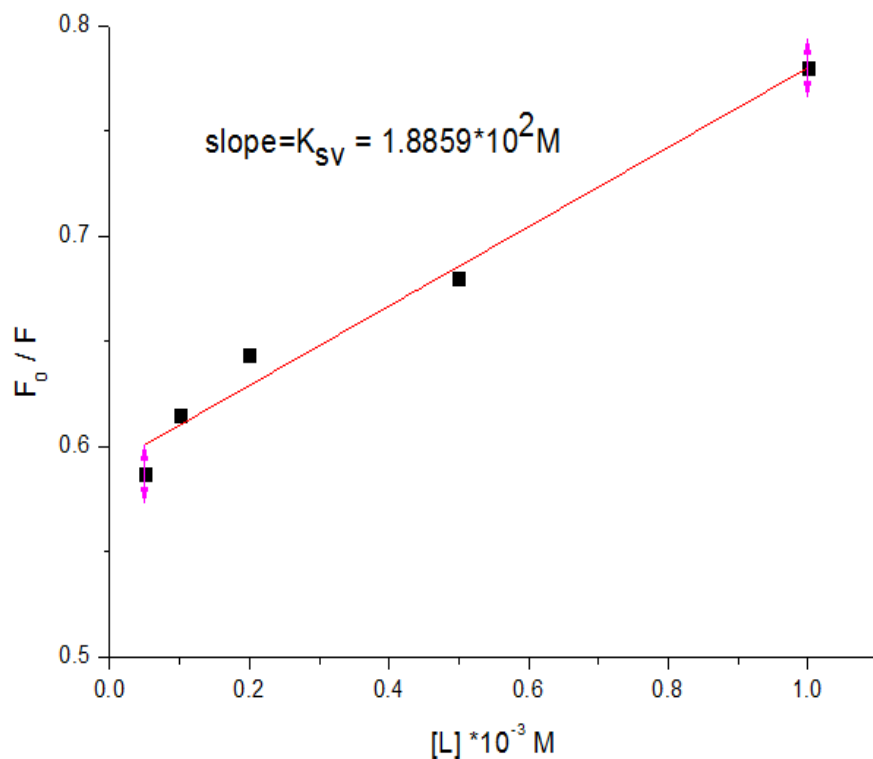


Figure 4.4: The plot of $\frac{F_0}{F}$ vs $[L]$ for HSA- Retinol

4.2.2. Determination of the binding constants (K) by fluorescence spectroscopy for HAS - Retinol:

For static quenching, the following equation is used to determine the binding constant between HSA and the drug.

$$\frac{1}{F_0 - F} = \frac{1}{F_0 K(L)} + \frac{1}{F_0} \quad (5)$$

Where K is the binding constant of drug with HSA. To determine the binding constants of HSA-Retinol systems, a plot of $\frac{1}{F_0 - F}$ vs $\frac{1}{L}$ for different Retinol concentrations is made. The plots are linear and have a slope of $\frac{1}{F_0 K}$ and intercept $\frac{1}{F_0}$ according to the above equation. By taking the quotient of the intercept and the slope, the binding constants K(L) can be calculated.

The plot of $\frac{1}{F_0 - F}$ vs $\frac{1}{L}$ for HSA- Retinol complexes are shown in (Fig 4.5). The binding constants for retinol with HSA have been calculated from the slope and the intercept in (Fig. 4.5) and are found to be $1.32 * 10^2 \text{ M}^{-1}$ for HSA- Retinol.

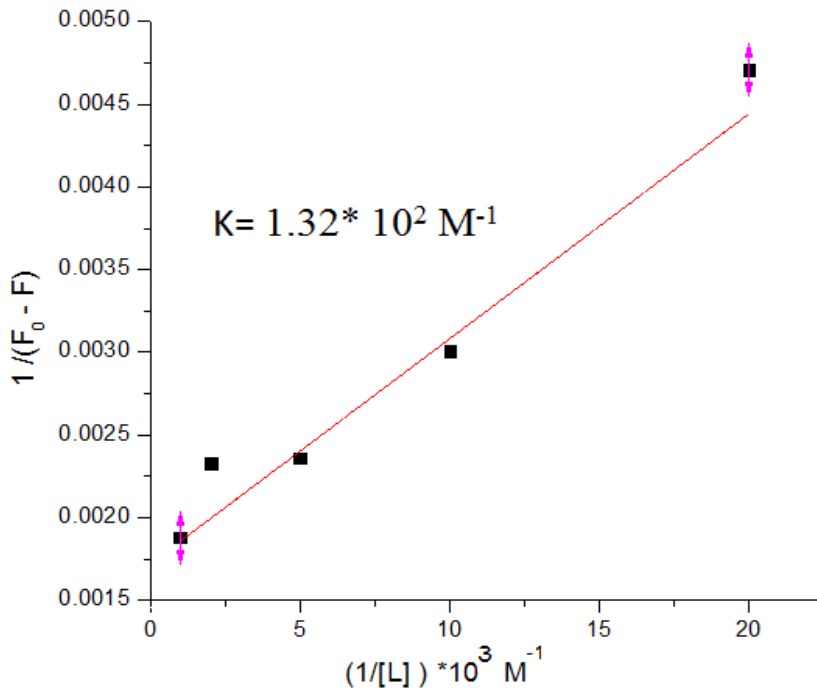


Figure 4.5: The plot of $\frac{1}{F_0 - F}$ vs $\frac{1}{L}$ for HSA- Retinol complexes.

4.3 FT-IR Spectroscopy

FT-IR spectroscopy is a good technique for the study of hydrogen bonding (Li, Y., et al 2006), and has been identified as one of the few techniques that is established in the determination of protein secondary structure at different physiological systems (Sirotkin, V., et al 2001; Surewicz, W.K., et al 1993; Arrondo, J., et al 1993). FT-IR spectroscopy provides information about the secondary structure content of proteins, unlike X-ray crystallography and NMR spectroscopy which provide information about the tertiary structure (Kendrew, J., et al 1958). FTIR spectroscopy works by shining infrared radiation on a sample and seeing which wavelengths of radiation in the infrared region of the spectrum are absorbed by the sample. Each compound has a characteristic set of absorption bands in its infrared spectrum. Characteristic bands found in the infrared spectra of proteins and polypeptides include the Amide I and Amide II. (Kong, J., & Yu, S. 2007; Byler, M., & Susi, H., 1986). Amide I band ranging from 1700 to 1600 cm^{-1} and arises principally from the C=O stretching (Vandenbussche, G., et al 1992), and has been widely accepted to be used (Workman, J., 1998). The amide II band is primarily N-H bending with a contribution from C-N stretching vibrations, amide II ranging from 1600 to 1480 cm^{-1} . And amide III band ranging from 1330 to 1220 cm^{-1} which is due to the C-N stretching mode coupled to the inplane N - H bending mode. (Goormaghtigh, E., et al 1990; Sirotkin, V., et al 2001). See figure 4.6.

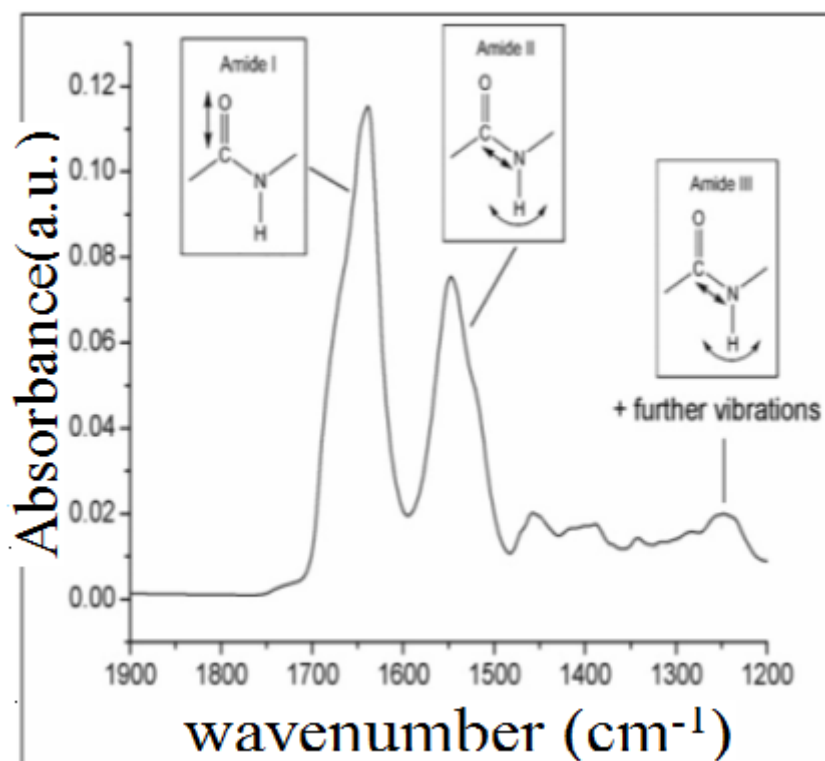


Figure 4.6: Sample spectrum showing the three relevant regions for determination of protein secondary structure. Amide I (1700-1600 cm^{-1}), amide II (1600-1480 cm^{-1}) and amide III (1330-1220 cm^{-1}) (Vonhoff, S., et al 2010).

4.3.1. Peak positions:

The spectra of second derivative of HSA free, where the major spectral absorbance of amide I band at 1657 cm^{-1} (mainly C=O stretch), and amide II band at 1543 cm^{-1} (C-N stretching coupled with N-H bending modes) as shown in Figure 4.7.

The spectrum of HSA- Retinol mixtures with different percentages of Retinol. It is seen as the Retinol ratios is increased, the intensity of amide I, amide II, amide III was decreased further in the spectra of all HSA- Retinol mixtures as shown in Figure 4.8. The reduction in the intensity of three amide bands is related to HSA- Retinol interactions (AbuTair, M., et al 2010).

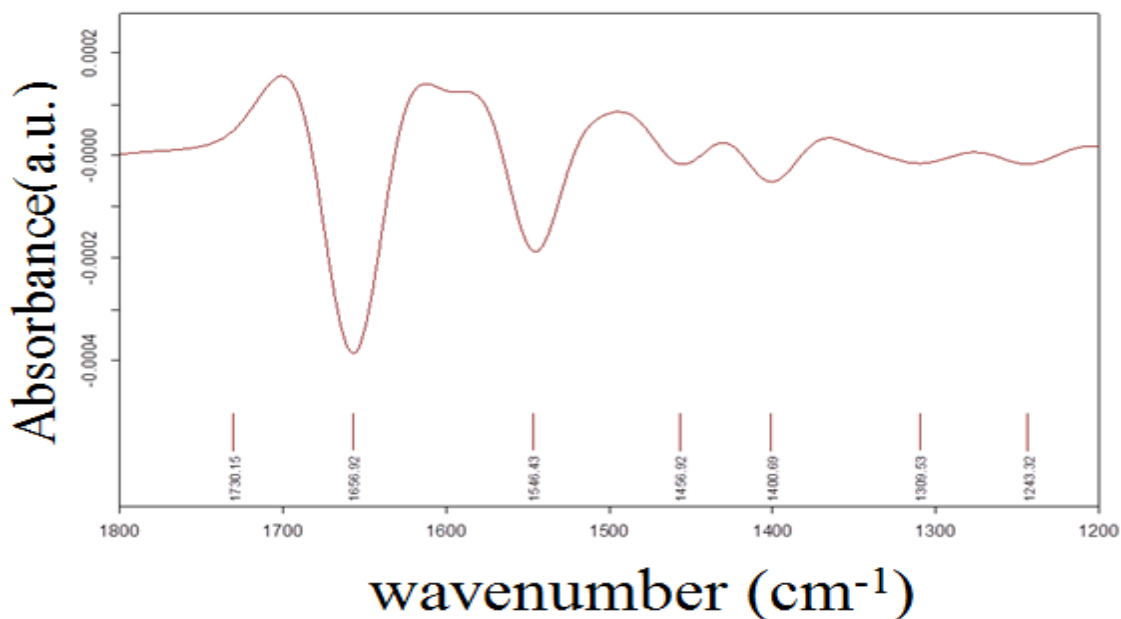


Figure 4.7: The spectra of HSA free (second derivative).

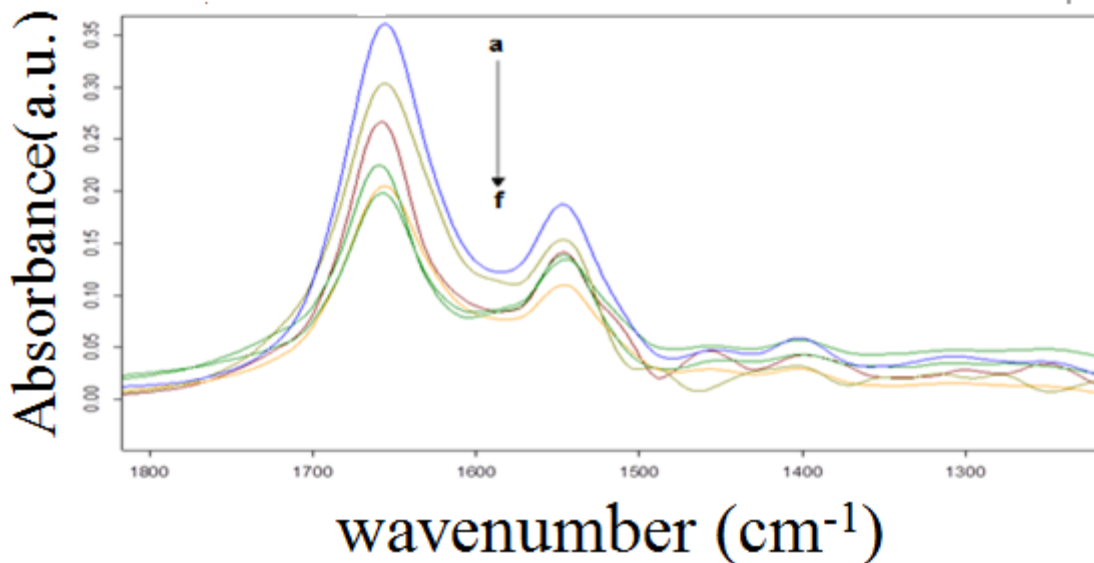


Figure 4.8: (a, b, c, d, e, f) Retinol -HSA with ratios (0:1, 1:1, 2:1, 5:1, 10:1, 20:1), respectively.

In table (4.1) the peak positions of HSA with different ratios of retinol are listed. For retinol - HSA interaction the amide bands of HSA infrared spectrum shifted as listed in the table ,

for **amide I** band the peak positions have shifted as follows: 1617 cm^{-1} to 1618 cm^{-1} , 1643 cm^{-1} to 1647 cm^{-1} , 1656 cm^{-1} to 1659 cm^{-1} , 1670 cm^{-1} to 1669 cm^{-1} , in addition new peaks have been appeared at high molecular ratios of retinol at 1535 cm^{-1} and 1587 cm^{-1} , And the peaks at 1693 cm^{-1} remains unchanged after the interaction.

In **amide II** the peak positions have shifted as follows: 1501 cm^{-1} to 1503 cm^{-1} , 1534 cm^{-1} to 1538 cm^{-1} , 1560 cm^{-1} to 1559 cm^{-1} , 1580 cm^{-1} to 1576 cm^{-1} , in addition new peaks have been appeared at high molecular ratios of retinol at 1522 cm^{-1} and 1594 cm^{-1} .

In **amide III** region the peak positions are also have been shifted as the following order: 1244 cm^{-1} to 1243 cm^{-1} , 1253 cm^{-1} to 1255 cm^{-1} , 1269 cm^{-1} to 1267 cm^{-1} , 1272 cm^{-1} to 1276 cm^{-1} , in addition new peaks have been appeared at high molecular ratios of retinol at 1329 cm^{-1} , And the peaks at 1298 cm^{-1} remains unchanged after the interaction.

Shifts in peak shape of certain elements can occur due to difference in chemical bonding, between different samples/standards. The shifts in peaks shape of HSA after the interaction with retinol has been occurred are due to the changes in protein secondary structure. Those shifts are attributed to the newly imposed hydrogen bonding between retinol (on both =O and -OH sites) and the protein (AbuTair, M., et al 2010; Sarver, R.W., & Krueger, W.C. 1991).

It has been observed for the retinol -HSA complexes in **amide I** band, that the shift to higher frequency for the second peak (1643-1647 cm^{-1}) and then for the major peak (1656-1659 cm^{-1}).

In **amide II** the higher shift occurs at the major peak (1534-1538 cm^{-1}).

The peak shift in **amide III** has been observed at (1272-1276 cm^{-1}).

Hydrogen bonding may affect the bond strength, may have impact on the IR, causing the peak shift, larger or smaller. In amide I the observed characteristic band shifts often allow the assignment of these bands to peptide groups or to specific amino-acid side-chains. An additional advantage is the shift of the strong water absorbance away from the amide I region (1610–1700 cm^{-1}) which is sensitive to protein structure. The minor but reproducible shift indicates that a partial unfolding of the protein occurs in HSA, with the retention of a residual native-like structure. It has been observed that the shifts in peaks are going toward a higher wave number, this implies that the strength of the bond has been increased but with a small percentage (Uversky, V.N., et al 2007).

Table 4.1: Band assignment in the absorbance spectra of HSA with different Retinol molecular ratios for amide I, amide II, and amide III region.

Bands	HSA Free	HSA- Vit.A ₁				
		1:01	1:02	1:05	1:10	1:20
Amide I (1600-1700)	1617		1616	1619	1618	1618
			1634	1634	1634	1635
	1643	1645	1647	1646	1647	1647
	1656	1657	1658	1658	1657	1659
	1670	1670	1670	1669	1669	1669
			1686	1686	1687	1687
Amide II (1480-1600)	1501	1501	1502	1503	1504	1503
			1522	1523	1523	1522
	1534	1537	1538	1538	1539	1538
	1560	1560	1559	1560	1559	1559
	1580	1580	1576	1574	1576	1576
				1595	1594	1594
Amide III (1220-1330)	1244	1242	1243	1243	1243	1243
	1253	1253	1254	1254	1255	1255
	1269	1269	1269	1268	1267	1267
	1272	1272	1274	1276	1276	1276
	1298	1297	1298	1298	1298	1298
			1329	1328	1329	1329

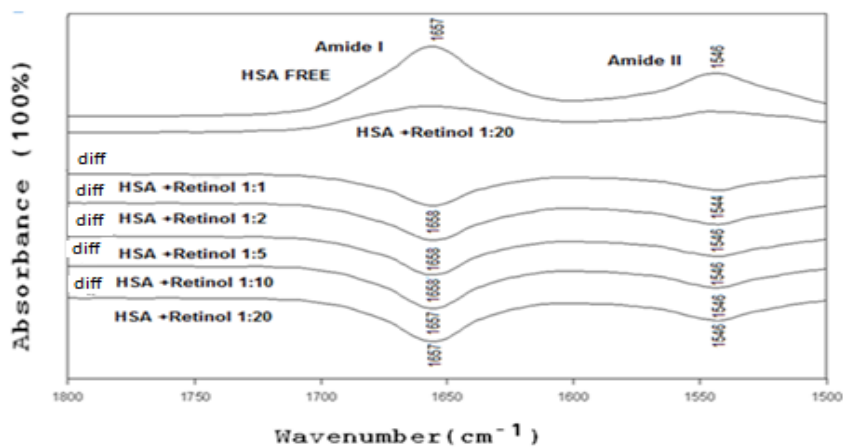


Figure 4.9: FTIR spectra (top two curves) and difference spectra [(protein solution+ Retinol solution)-(protein solution)] (bottom five curves) of the free human serum albumin (HSA) and its Retinol complexes in aqueous solution.

4.3.2 Secondary structural changes:

The Determination of the secondary structure of HSA and its retinol complexes were carried out on the basis of the procedure described by Byler and Susi (Byler, M., & Susi, H., 1986). In this work a quantitative analysis of the protein secondary structure for the free HSA, and Retinol – HSA complexes in dehydrated films are determined from the shape of Amide I, II and III bands. Baseline correction was carried out in the range of (1700–1600 cm^{-1}), (1600-1480 cm^{-1}), and (1330–1220 cm^{-1}) to get amide I, II, and III bands.

Then Fourier self-deconvolution and second derivative were applied to these three ranges respectively to increase spectral resolution and therefore to estimate the number, position and the area of each component bands. Based on these parameters curve-fitting process was carried out by Opus software (version 5.5) to obtain the best Lorentzian-shaped curves that fit the original HSA spectrum. The individual bands are identified with its representative secondary structure, and the content of each secondary structure of HSA is calculated by area of their respective component bands. The procedure was in general carried out considering only components detected by second derivatives and the half widths at half height (HWHH) for the component peaks are kept around 5 cm^{-1} (Darwish, S.M. et al. 2012).

The component bands of amide I were attributed according to the well-established assignment criterion (Jiang, M., et al, 2004; Ivanov, A. et al 1994). **Amide I** band ranging from 1610 to 1700 cm^{-1} generally assigned as follows 1610–1624 cm^{-1} are generally represented to β -sheet, 1625–1640 cm^{-1} to random coil, 1646–1671 cm^{-1} to α -helix, 1672–1787 cm^{-1} to turn structure, and 1689-1700 cm^{-1} to β -ant parallel (Lin, S.Y. 2003; Szabo, Z. et al.1999; Cerf, E. et al. 2009).

For **amide II** ranging from 1480 to 1600 cm^{-1} , the absorption band assigned in the following order: 1488–1504 cm^{-1} to β -sheet, 1508–1523 cm^{-1} to random coil, 1528–1560 cm^{-1} to α -helix, 1562–1585 cm^{-1} to turn structure, and 1585-1598 cm^{-1} to β -ant parallel.

And for **amide III** ranging from 1220 to 1330 cm^{-1} have been assigned as follows: 1220–1256 cm^{-1} to β -sheet, 1257–1285 cm^{-1} to random coil, 1287–1301 cm^{-1} to turn structure, and 1302–1329 cm^{-1} to α -helix (Li, H. et al. 2009).

Most investigations have concentrated on Amide I band assuming higher sensitivity to the change of protein secondary structure (Vass, E., et al 1997). However, it has been reported that amide II and amide III bands have high information content and could be used for prediction of proteins secondary structure (Oberg, K., et al 2004; Xie, M., et al 2003; Jiang, M., et al 2004; Liu, Y., et al 2003).

Based on the above assignments, the percentages of each secondary structure of HSA were calculated from the integrated areas of the component bands in Amide I, II, and respectively. Where the area of all the component bands assigned to a given conformation is then summed and divided by the total area. The obtained number is taken as the proportion of the polypeptide

chain in that conformation. The Secondary structure determination for the free HSA and its retinol mixture with different retinol concentrations are given in (Table 4.2). The second derivative resolution enhancement and curve – fitted Amide I and secondary structure determinations of the free human serum albumin (A, B) and its retinol mixture (C, D) with the highest concentrations in dehydrated films are shown in (Figure 4.10). It is generally accepted that infrared spectra of proteins in films and in solution may display distinct differences, but these differences are due to the presence or absence of the water or buffer molecules that imprint their mark on the spectra. It has been shown that the structural information content is of the same quality in films and in solution with an (error of < 1%) for both systems (Ahmed Ouameur, A., et al. 2004).

In amide I region, the free HSA contained major percentages of:

α -helical (49%).

β - sheet (16%)

Random coil (10 %).

β -turn structure (14%).

Anti-parallel β - sheet (11%)

As a result of HSA- Retinol mixture:

α -helical structure reduced from 49% to 32% at 20:1 molecules Retinol to HSA .

β -sheet increased from 16% to 24% at 20:1 molecules Retinol to HSA.

Random coil increased from 10% to 17% at 20:1 molecules Retinol to HSA.

β -turn structure reduced from 14% to 11% at 20:1 molecules Retinol to HSA.

Antiparallel β -sheet increased from 11% to 16% at 20:1 molecules Retinol to HSA.

In amide II region, the free HSA contained

α -helical (46%).

β -sheet (24%).

Random coil (10 %).

β -turn structure (9%).

Anti β - sheet (11%)

As a result of HSA- Retinol mixture:

α -helical structure reduced from 46% to 33% at 20:1 molecules Retinol to HSA

β -sheet increased from 24% to 31% at 20:1 molecules Retinol to HSA

Random coil increased from 10% to 13% at 20:1 molecules Retinol to HSA

β -turn structure reduced from 9% to 6%. At 20:1 molecules Retinol to HSA

Anti β -sheet increased from 11% to 17% at 20:1 molecules Retinol to HSA

In amide III region, HSA free contained:

α -helical (47%)

β -sheet (32%)

Random coil (10%)

β -turn structure (11%).

As a result of HSA – Retinol mixture:

α -helical structure reduced from 47% to 40% at 20:1 molecules Retinol to HSA

β -sheet increased from 32% to 38% at 20:1 molecules Retinol to HSA

Random coil increased from 10% to 13% at 20:1 molecules Retinol to HSA

β -turn structure decreased from 11% to 8% at 20:1 molecules Retinol to HAS

The reduction of α -helix intensity percentage in favor of the increase of β -sheets percentage are believed to be due to the unfolding of the protein in the presence of Retinol as a result of the formation of H bonding between HSA and the Retinol mixture. The newly formed H-bonding result in the C–N bond assuming partial double bond character due to a flow of electrons from the C=O to the C–N bond which decreases the intensity of the original vibrations (Chirgadze, Y., et al 1975; Jackson, M., et al 1991). It seems that the H-bonding affects more of the original bonding in α - helix than in β -sheets depending on the accessibility of the solvent and on propensities of α - helix and β -sheets of the HSA (Parker, S., 1983), as discussed in chapter two the hydrogen bonds in α -helix are formed inside the helix and parallel to the helix axis, while for β -sheet the hydrogen bonds take position in the planes of β -sheets as the preferred orientations especially in the anti-parallel sheets, so the restrictions on the formation of hydrogen bonds in β -sheet relative to the case in α helix explains the larger effect on reducing the intensity percentage of α -helix to that of β -sheet (Darwish, S. M., et al 2010; Holzbaur, I., et al 1996; Zhang, W., et al 1999). Similar conformational transitions from a α -helix to β -sheet structure were observed for the protein unfolding upon protonation and heat denaturation (Beauchemin, R., et al, 2007; Surewicz, W.K., et al 1993 ; Holzbaur, I., et al 1996; Parker, S., 1983). These results indicate Retinol interact with HSA through C=O and C-N groups in the HSA polypeptides. The Retinol – HSA mixture caused the rearrangement of the polypeptide carbonyl hydrogen bonding network and finally the reduction of the protein α -helical structure.

Table 0.2: Secondary structure determination for the free HSA and its Retinol mixture for amide I, amide II, amide III.

2 nd Structure	HSA Free (%)	HSA- V.A ₁ 1:1 (%)	HSA- V.A ₁ 1:2 (%)	HSA- V.A ₁ 1:5 (%)	HSA- V.A ₁ 1:10 (%)	HSA- V.A ₁ 1:20(%)
Amide I						
β - sheets (cm ⁻²) (1610-1624)	16	19	14	18	19	24
Random (cm ⁻²) (1625-1640)	10	14	15	17	16	17
α - hilex (cm ⁻²) (1646-1671)	49	43	41	39	35	32
Turn (cm ⁻²) (1672-1687)	14	11	13	11	13	11
Anti β - sheets (cm ⁻²) (1689-1700)	11	13	17	15	17	16

Amide II						
β - sheets (cm ⁻²) (1488-1504)	24	28	26	29	30	31
Random (cm ⁻²) (1508-1523)	10	13	15	13	12	13
α - hilex (cm ⁻²) (1528-1560)	46	38	34	32	33	33
Turn (cm ⁻²) (1562-1585)	9	8	9	8	7	6
Anti β - sheets (cm ⁻²) (1585-1598)	11	13	16	18	18	17
Amide III						
β - sheets (cm ⁻²) (1220-1256)	32	37	35	38	39	38
Random (cm ⁻²) (1257-1285)	10	15	15	14	13	13
Turn (cm ⁻²) (1287-1301)	11	11	11	10	10	8
α - hilex (cm ⁻²) (1302-1329)	47	37	39	38	38	40

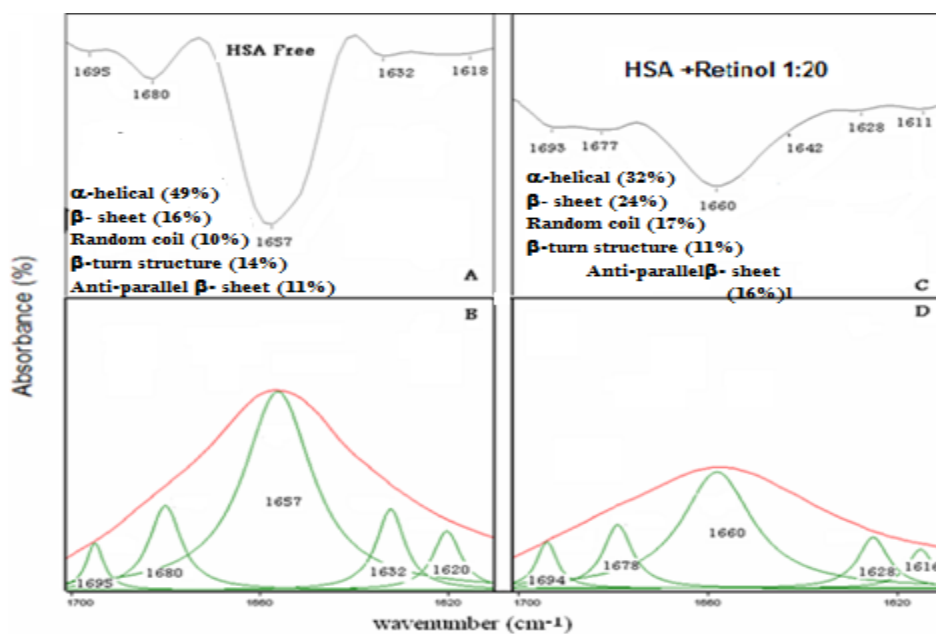


Figure 4.10 Second-derivative enhancement and curve-fitted Amide I region (1600-1700 cm⁻¹) and secondary structure determination of the free human serum albumin (A and B) and its Retinol mixture(C and D) with 20: Retinol: HSA ratios.

Chapter Five

Conclusions and future work

Conclusions and future work

In this work, the interaction between Retinol (vitamin A₁) and HSA Albumin (the universal hydrophobic molecule carrier) has been investigated using spectroscopic techniques, including (FT-IR, Fluorescence and UV-VIS spectrophotometers). Our experimental work showed relatively high binding affinity between Retinol and HSA. Referring to UV spectrum, the calculated binding constant for Retinol - HSA is ($K = 1.717 \times 10^2 \text{ M}^{-1}$). The analysis of fluorescence spectrum yield binding constant for Retinol -HSA interaction, it has been measured to be ($K = 1.32 \times 10^2 \text{ M}^{-1}$). The binding constant obtained by different methods has very close values. The value of Stern-Volmer quenching constant and quenching rate constant for Retinol have been measured to be ($K_{sv} = 1.885 \times 10^2 \text{ M}$, $K_q = 1.885 \times 10^{10} \text{ L Mol}^{-1}\text{s}^{-1}$). These experimental results show that static quenching is responsible for the fluorescence quenching (decrease of intensity). This is an indication for complex formation between the protein and Retinol.

Analysis of FT-IR spectrum indicate that increasing the concentration of Retinol lead to the unfolding of protein, decreasing the percentage of the α -helical structure in favor of β -sheet structure (Uversky, V.N., et al . 2007). Beside that it can be inferred that the binding forces which are involved in the binding process includes hydrophobic interactions. The newly formed H-bonding result in the C–N bond assuming partial double bond character due to a flow of electrons from the C=O to the C–N bond which decreases the intensity of the original vibrations (Sarver, R.W., et al 1991).

The binding study of Retinol with HSA is of great importance in pharmacy, pharmacology and biochemistry. This research can supply some important information to clinical research and provide the theoretical basis for new Retinol designing. Therefore, this research need further studies to be a useful guide for synthesis of efficient Retinol such as the determinations of binding sites, binding location, and thermodynamic parameters (enthalpy ,free energy ,entropy) at different temperatures to deduce the type of the acting force for the binding reaction between Retinol and HSA.

Further investigations are recommended to be held in the field of temperature effect upon Retinol -Human serum interaction, and how does the protein structure will differ with temperature change.

References

- *Abou-Zied, K., and Al-Shishi, O., (2009). Journal of the American Chemical Society, 130, p10793.*
- *Abu Tair, M., Ghithan s, J., Darwish , M., Abu-hadid, M., (2010). Journal of Applied Biological Sciences 5 (13): 35-47.*
- *Abu Teir, M. M., Ghithan J., Abu-Taha M. I.I, Darwish S. M., Abu-hadid M. M..(2014). Journal of Biophysics and Structural Biology. 6(1).1-12.*
- *Ahmed Quamour, A., et al. (2004). Biopolymers, 73, p503. Berg, J., and Stryer, L., (2001): Biochemistry, 5th ed, NewYork.*
- *Arrondo, J., and Muga, A., (1993). Prog. Biophys. Mol. Biol., 59, p23.*
- *Aruldas, G. (2007). Molecular structure and spectroscopy, 2nd ed., PHI learning private limited, New Delhi.*
- *Bai, Y., and Nussinov, R. (2007). Protein Folding Protocols, Humana Press Inc.*
- *Ball, D.W. (2001). The basics of spectroscopy, SPIE- the international society for*
- *Banwell, C. N.(1972): Fundamentals of Molecular Spectroscopy. 2nd ed., McGRAW-HILL Bokk Company (UK) Limited.*
- *Bates, C.J. Vitamin A. The Lancet 1995;345:31-35.*
- *Beauchemin, R., et al. (2007). Biomacromolecules 8, p3177.*
- *Beharka, A., Redican, S., Leka, L., Meydani, S., (1997). Methods Enzymol, 282, 247-263.biochemistry, Plenum Press, New York.*
- *Bhattacharya, A., Gruene, T., Curry, S.(2000). Crystallographic Analysis Reveals Common Modes of Binding of Medium and Long-chain Fatty Acids to Human Serum Albumin. J. Mol. Biol,303, P 721-732).*
- *Buxbaum, E. (2011). Biophysical chemistry of proteins: an introduction to laboratorymethod, springer science+ Business media. LLC.*
- *Byler, M., and Susi, H., (1986). Biopolymers, 25, p469.*
- *Carter, Xiao-MinHe, Sibyl H. Munson, Pamela D. Twigg, Kim M.Gernert, M. Beth Broom,TeresaY. Miller. (1989) .Three-Dimensional Structure of Human Serum. The Space Science Laboratory, ES76 Biophysics, Marshall Space Flight Center, USA. Daniel C.*
- *Cerf, E. et al. (2009). Biochem.J. 421, pp415-423.*
- *Cheng, F. Q., Wang, Y. P., Li, Z.P., Chuan, D. (2006). Spectrochimica Acta Part A, 65, p144.*
- *Chirgadze, Y., Fedorov, O., Trushina, N., (1975). Biopolymers 14, p679.*
- *Colin, D.(2014): Introduction to Protein Structure Prediction. www.biostst.wisc.edu/bmi776/*
- *Cooper, A. (2004). Biophysical Chemistry, The Royal Society of Chemistry, UK.*
- *Cui,A., Lixia Qin, A., Guisheng, Z.A., Xiaobing, L.A., Xiaojun,Y.B., Beilei ,L.B . (2008). A concise approach to 1,11-didechloro-6-methyl-40-O-demethyl rebeccamycin and its binding to human serum albumin: Fluorescence spectroscopy and molecular modeling method Fengling. Bioorganic & Medicinal Chemistry,16,7615–7621.*
- *Darwish, S. M., Abu sharkh, S. E., Abu Teir, M. M., Makharza, S. A., Abu-hadid, M.M.. (2010). Journal of Molecular Structure, 963, p122–129.*

- Darwish, S.M. et al. (2012), *spectroscopic investigation of pentobarbital interaction with Transthyretin*, vol 2013, p10, *journal of spectroscopy*.
- Goormaghtigh, E., Cabiaux, V., Ruysschaert, J., (1990). *European Journal of Biochemistry*, 193, p409.
- Gorga, F.R.(2007): Introduction to Protein Structure. Bridgewater State College. <http://webhost.bridgew.edu/fgorga/proteins/>
- Griffiths, P. and Haseth, J. (2007): *Fourier Transform Infrared Spectrometry. 2nd ed, John Wiley & Sons-Hoboken, New Jersey*.
- Gropper, S. S., Smith, J. L., Groff, J. L. (2009): *Advanced Nutrition and Human Metabolism*. 5th ed. Canada: Wadsworth Cengage Learning.
- Haris , P. I., Severcan, F. (1999). *Journal of Molecular Catalysis B: Enzymatic*, 7 , P 207.
- Hildebrandt, P., Siebert, F.(2008): *Vibrational Spectroscopy in Life Science, 1st, John Wiley & Sons Ltd,UK*.
- Hollas, J. (2004): *Modern Spectroscopy, 4th, John Wiley & Sons Ltd, UK*.
- Holzbaur, I., English, A., Ismail, A., (1996). *Biochemistry* 35, p5488.
- IUPAC, Compendium of Chemical Terminology, 2nd ed. (the "Gold Book") (1997). Online corrected version: (2006–) "hydrophobic interaction".
- Ivanov, A. et al. (1994). *Journal of Applied Spectroscopy*, 60, p305.
- Jackson, M., and Mantsch, H., (1991). *J. Chem.*, 69, p1639.
- Jiang, M., Xie, M., Zheng, D., Liu, Y., Li, X., Chen, X., (2004). *Journal of Molecular Structure*, 692, p71.
- Ji-Sook, Ha.A., Theriault,A.C., Nadhipuram,V., Bhagavan A., Chung-Eun Ha.B.. (2006). Fatty acids bound to human serum albumin and its structural variants modulate apolipoprotein B secretion in HepG2 cells. *Biochimica et Biophysica Acta* 1761 (2006) 717–724)
- Kalsi, P.S. (2004). *Spectroscopy Of Organic Compounds*, 6th ed., New Age international publishers Ltd.
- Kandagal ,P.B., Shaikh, S.M.T., Manjunatha, D.H., Seetharamappa, J., Nagaralli, B.S..(2007).Spectroscopic studies on the binding of bioactive phenothiazine compounds to human serum albumin. *J. Photochem. Photobiol. A* 189, P 121-127.
- Kang, J., Liu, Y., Xie, M.X., Li, S., Jiang, M., Wang, Y.D. (2004). Interactions of human serum albumin with chlorogenic acid and ferulic acid. *Biochimica et BiophysicaActa* ,1674, P 205– 214.
- Kendrew, J., Bodo, G., Dintzis, H., Parrish, R., Wyckoff, H., Philips, D., (1958). *Nature* 18, 662-666.
- Klotz, M.I., Hunston, L.D. (1971). *Biochemistry*, 10, P 3065.
- Kong, J., and Yu,S. (2007). *Acta Biochimica et Biophysica Sinica*, 39(8), 549–559.
- Kragh-Hansen, U., (1981). *Pharmacol. Rev.*, 33, p17.
- Krishnakumar, S.S., Panda, D. (2002). *Biochemistry*,41, P7443.
- Lakowicz, J.R. (2002). *Topics in fluorescence spectroscopy, Vol 5, Kluwer academic publishers*.
- Lakowicz, J.R., (2006): *Principles of Fluorescence Spectroscopy, 3rd ed, Springer Science+Business Media, USA*.

- Lammer EJ, Chen DT, Hoar RM. Retinoic acid embryopathy. *N Eng J Med* 1985;313:837-841.
- Li, H. et al. (2009). Amyloid and protein aggregation – analytical method, John Wiley and sons, pp 1-32.
- Li, Y., Ying, He,W., Ming, D., Shenga, F., Zhi,D.(2006). Human serum albumin interaction with formononetin studied using fluorescence anisotropy, FT-IR spectroscopy, and molecular modeling methods .*Bioorganic & Medicinal Chemistry*,14,P 1431–1436.
- Lin, S.Y. (2003). *International Journal of Biological Macromolecules*. 32, pp173-177.
- Litwack. G, Axelord. J. (1970): Binding of Hormones to Serum Proteins. *Biochemical Actions of Hormones*. Volume.1. New York: Academic Press, INC. p 209-260.
- Liu, Y., Xie, M., Kang, J., Zheng, D., (2003). *Spectrochim. Acta, Part A*, 59, p2747.
- Mirabeela, F.M. (ED) (1998): *Modern Techniques in Applied Molecular Spectroscopy*, John Wiley & Sons Ltd,UK.
- Morse, P. M. (1929). "Diatomic molecules according to the wave mechanics. II. Vibrational levels". *Phys. Rev.* 34. pp. 57–64.
- *NanoDop 3300 Fluorospectrometer V2.7 user's Manual, 2008, Thermo Fisher Scientific.*
- *NanoDrop 1000 Spectrophotometer V3.7, User's Manual, 2008, Thermo Fisher Scientific.*
- Narhi, L.O. (2013): *Biophysics for Therapeutic protein Development*, 1st, Springer Science + Business media, USA.
- Neault, J.F., and Tajmir-Riahi, H.A.(1998). *Biochimica et Biophysica Acta*, 1384, p153.
- Nelson DL, Cox MM (2005). *Lehninger's Principles of Biochemistry* (4th ed.). New York, New York: W. H. Freeman and Company.
- Norman, A.W., Mizwicki, M.T., Norman, D.P..(2004). *Nature Reviews: Steroid-Hormones Rapid Actions, Membrane Receptors and a Conformational Ensemble model*. *Nature Reviews*. Volume 3.
- Oberg, K., Ruyschaert, J., Goormaghtigh, E., (2004). *Eur. J. Biochem.*, 271, p2937.
- optical engineering.
- *OPUS bruker manual version 5.5, 2004 BRUKER OPTIK GmbH. Nikolić, G. S. (2011): Fourier Transforms - New Analytical Approaches and FT-IR Strategies, InTechJanezaTrdine 9, 51000 Rijeka, Croatia.*
- Ouameur,A., Mangier,S., Diamantoglou, R., Rouillon, R., CarpentierH. A., Tajmir, R.. (2004). *Effects of Organic andInorganic Polyamine Cationson the Structure of HumanSerum Albumin. Biopolymers, Vol. 73, 503–509*
- Parker, S., (1983): *Applications of infrared, raman, and resonance raman spectroscopy in*
- Pavis, D. et al. (2008). *Introduction to spectroscopy*. 4th ed., cengage learning.
- Purcell, M., Neault J., Tajmir-Riahi, H., (2000). *Biochimica et Biophysica Acta*, 1478, p61.
- Raaman, N. (2006). *Phytochemical Techniques*, New India publishing agency.
- Reece, J. B., Urry, A. L., Cain,L. M., Wasserman, A.S., Minorsky,V.P., Jackson, B. R.(2011): *Campbell Biology*. Pearson Benjamin Cummings, 9th ed. USA.
- Richardson, J.S.(2007): *The Anatomy and Taxonomy of Protein Structure*. DukeUniversity.<http://kinemage.biochem.duke.edu/teaching/anatax/index.html>

- Rondeau, P.A., Armenta,S.B., Caillens, H.C., Chesne, S.A., Bourdon, E.A.. (2007). Assessment of temperature effects on b-aggregation of native and glycosylated albumin by FT-IR spectroscopy and PAGE: Relations between structural changes and antioxidant properties. *Archives of Biochemistry and Biophysics*,460, P141–150.
- Rosman, B. (2008). Calculation of Molecular Vibrational Normal Modes./www.homepages.inf.ed.ac.uk/
- Sarver, R.W., Krueger, W.C. (1991). Protein secondary structure from fourier transform infrared spectroscopy: a data base analysis, Vol. 194, 89-100.
- Schulman, S.G. (1977). Fluorescence and phosphorescence spectroscopy: physiochemical principles and practice, Vol 59, A. Wheaton & Co. Ltd, Exeter.
- Sharma, B.K. (2007). Spectroscopy. 20th ed., Goel Publishing house, Meerut, Delhi.
- Sheehan, D. (2009). Physical Biochemistry: principles and applications. 2nd ed., JohnWiley & sons Ltd.
- Shernan, M. (2014). Infrared Spectroscopy: A Key to Organic Structure, Yale-New Haven Teachers Institute.
- Sirotkin, V., Zinatullin, A., Solomonov, B., Faizullin, D., Fedotov, V.,(2001). *Biochimica et Biophysica Acta*, 1547, p359.
- Smith, FR, Goodman DS. Vitamin A transport in human vitamin A toxicity. *N Eng J Med* 1976;294:805-808.
- Smith, B.C. (2011), Fundamentals of Fourier Transform Infrared Spectroscopy, 2nded.,CRC press, Taylor and Francis Group LLC.
- Sommer A. Vitamin A Deficiency and Clinical Disease: An Historical Overview. *J Nutr* 2008;138:1835-1839.
- Stephanos, J., Farina, S., Addison, A.(1996). *Biochem.Biophys.Acta*, 1295,p 209-221.
- Stuart, B. (2004). Infrared spectroscopy fundamentals and applications,ANTS.
- Stuart, B. (1997): Biological Applications of Infrared Spectroscopy,1st, John Wiley & Sons Ltd,UK.
- Sulkowaska, A., (2002), *J. Mol. Struct.*, 614, p227.
- Surewicz, W., Moscarello, M., Mantsch, H., (1987). *J. Biol. Chem.*, 262, p8598.
- Surewicz, W.K., Mantsch, H.H., Chapman, D. (1993). *Biochemistry*,32, P 389.
- Szabo, Z. et al. (1999). *Biochemical and Biophysical Research Communications* 265, 297–300.
- Xiao-Min-He, Daniel C. Carter. Atomic Structure and Chemistry of Human Serum Albumin.Vol 358.16 July 1992.
- Turro, N.J. (1991). Modern Molecular Photochemistry, University science books, America.
- Tushar,K.M., Kalyan,S.G., Anirban,S., Swagata,D., (2008). The interaction of silibinin with human serum albumin:A spectroscopic investigation. *Journal of Photochemistry and Photobiology A: Chemistry* 194 (297–307),
- Uversky, V.N., Permykov, A.E. (2007): *Methods in Protein Structure and Stability Analysis; Vibrational spectroscopy*, Nova Science Publishers, Inc, Hauppauge, New York.
- Vandenbussche, G., Clercx, A., Curstedt, T., Johansson, J., Jornvall, H., Ruyschaert, J., (1992). *European Journal of Biochemistry*, 203, p201.

- Vass, E., Holly, S., Majer, Zs., Samu, J., Laczko, I., Hollosi, M., (1997). *Journal of Molecular Structure*, 47, p408.
- Vonhoff, S., Condliffe, J., Schiffter, H., (2010). *Journal of Pharmaceutical and Biomedical Analysis*, 51, p39.
- Wang, T., Xiang, B., Wang, Y., Chen, C., Dong, Y., Fang, H., Wang, M. (2008). *Colloids Surf.B*, 65, P113.
- Whitford, D. (2005): *Proteins Structure and Function*. England: John Wiley & Sons Ltd.
- Williams, D. (1976), *methods of experimental physics: spectroscopy*, vol 13, part A, Academic press Inc.
- Wilson, E., Decius, J., Cross, P. (1955): *The Theory of Infrared and Raman Vibrational Spectra*, McGraw-Hill, New York.
- Workman, J., (1998): *Applied Spectroscopy: Optical Spectrometers*, Academic Press, San Diego.
- Xie, M., and Liu, Y., (2003). *Chem. J. Chin. Univ.*, 24, p226.
- Yadav, L.D. (2005). *Organic spectroscopy*, Klower academic publisher, New Delhi, India.
- Zhang, G., Que, Q., Pan, J., Guo, J..(2008). *Study of the interaction between icariin and human serum albumin by fluorescence spectroscopy. Journal of molecular structure* 881, P 132-138.
- Zhang, W., Li, A., (1999): *Medical Chemistry*, Higher Education Press.
- Kauppinen, J. K., D. J. Moffatt, H. H. Mantsch, and D. G. Cameron. 1981. Fourier self-deconvolution: a method for resolving intrinsically overlapped bands. *Appl. Spectrosc.* 35:271-276.
- Peng, L., Minboa, H., Fang, C., Xi, L., Chaocan, Z. (2008). *Protein & Peptide Letters*, 15, P360.

دراسة تأثير ريتينول على الالبوماين البروتين الناقل في بلازما الدم بواسطة تقنيات مطيافية الجزيئات.

اسم الطالب : رزق سلمان درابيع.

اسم المشرف الاستاذ. دكتور موسى ابو طير.

الملخص

إن توزيع وعمليات الأيض لكثير من العناصر البيولوجية في الجسم سواء كانت أمصال أو منتجات طبيعية، مرتبطة بقدرة هذه العناصر على الارتباط مع بروتين الدم البشري (HSA). إذا دراسة ارتبط مثل هذه الجزيئات مع بروتين الدم البشري له أهمية أساسية، وتوجد دراسات واسعة من جوانب مختلفة لتفاعلات الريتينول (فيتامين A₁) و بروتين الدم البشري (HSA) قيد التقدم بسبب أهميتها للعمليات السريرية. في هذه الدراسة. تم التحقق من التفاعل بين الريتينول و بروتين الدم البشري (HSA) باستخدام جهاز مطياف الأشعة فوق البنفسجية (UV- VIS Spectrophotometer) وجهاز انبعاث الاشعاع (Fluorescence spectroscopy) وجهاز مطياف تحويل فوريير للأشعة تحت الحمراء (FT-IR) و ثابت الترابط (Binding Constant) والآثار على بنية البروتين الثانوية (protein secondary structure).

تم حساب قيمة ثابت الترابط (Binding Constant) بين الريتينول (فيتامين A₁) و بروتين الدم البشري (HSA) عن طريق جهاز مطياف الأشعة فوق البنفسجية وجهاز مطياف انبعاث الاشعاع عند درجة حرارة الغرفة (293K) ووجدت كالتالي: $(1.717 \times 10^2 \text{M}^{-1})$ و $(1.32 \times 10^2 \text{M}^{-1})$ على التوالي، بالإضافة الى ذلك تم حساب ثابت (Stern-Volmer) وثابت (quenching rate): $(1.885 \times 10^2 \text{L M}^{-1})$ و $(1.885 \times 10^{10} \text{L Mol}^{-1} \text{s}^{-1})$. أظهر جهاز مطياف الأشعة فوق البنفسجية ان زيادة في كثافة الامتصاص مع زيادة النسب الجزيئية من الريتينول (فيتامين A₁) الى بروتين الدم البشري (HSA) ، مع بقاء تركيز بروتين الدم البشري (HSA) ثابت. ومن خلال استخدام جهاز انبعاث الاشعاع وجد أن شدة الاشعاع المنبعث نتيجة تفاعل الريتينول (فيتامين A₁) مع بروتين الدم البشري (HSA) تزداد بزيادة تركيز الريتينول (فيتامين A₁) مع بقاء تركيز البروتين (HSA) ثابت، حيث أن هذا الانخفاض في شدة الإشعاع المنبعث يشير إلى الريتينول (فيتامين A₁) لديه قدرة قوية على خفض او التقليل من الإشعاع المنبعث ذاتيا من بروتين الدم البشري (HSA) من خلال الية (static quenching).

باستخدام جهاز مطياف تحويل فوريير للأشعة تحت الحمراء (FT-IR) مع تطبيق تقنية (Fourier Self-deconvolution) و (Second Derivative resolution) وتقنية (curve fitting) تم تحليل مناطق أميد 1 و أميد 2 و أميد 3 في بروتين الدم البشري لتحديد بنية البروتين الثانوية (Secondary Structure) والية ارتباط ريتينول مع بروتين الدم، لقد لوحظ أنه مع زيادة تراكيز ريتينول إلى بروتين الدم فإن شدة حزم الامتصاص (Absorption bands) تقل.

أيضا جميع مواقع القمم (Peaks) تم تحديدها عند عدة نسب من ريتينول بالمقارنة مع بروتين الدم البشري. إضافة إلى ذلك أظهر الطيف المقاس بواسطة جهاز مطياف تحويل فوريير للأشعة تحت الحمراء أن البنية الثانوية لبروتين الدم البشري، تغيرت نتيجة إضافة نسب من ريتينول ، الذي ظهر في انخفاض في شدة حزم الامتصاص الممثلة ل (α -helix) بالمقارنة مع حزم الامتصاص الممثلة ل (β -sheets)، هذا التباين والاختلاف في الشدة يرجع الى تكوين الروابط الهيدروجينية (H-bonding) في الجزيئات المعقدة، وهو ما يفسر الميل الذاتي لكل من (α -helix) و (β -sheets) لتكوين هذه الروابط.